



# Growth of the continental crust induced by slab rollback in subduction zones: Evidence from Middle Jurassic arc andesites in central Tibet

Wan-Long Hu <sup>a,b</sup>, Qiang Wang <sup>a,b,c,\*</sup>, Jin-Hui Yang <sup>d</sup>, Lu-Lu Hao <sup>a,b</sup>, Jun Wang <sup>a,b</sup>, Yue Qi <sup>a,b</sup>, Zong-Yong Yang <sup>a,e</sup>, Peng Sun <sup>a</sup>

<sup>a</sup> State Key Laboratory of Isotope Geochemistry, Guangzhou Institute of Geochemistry, Chinese Academy of Sciences, Guangzhou 510640, China

<sup>b</sup> CAS Center for Excellence in Deep Earth Science, Guangzhou 510640, China

<sup>c</sup> College of Earth and Planetary Sciences, University of Chinese Academy of Sciences, Beijing 100049, China

<sup>d</sup> Institute of Geology and Geophysics, Chinese Academy of Sciences, Beijing 100029, China

<sup>e</sup> State Key Laboratory of Ore Deposit Geochemistry, Institute of Geochemistry, Chinese Academy of Sciences, Guiyang 550002, China

## ARTICLE INFO

### Article history:

Received 17 August 2022

Revised 28 November 2022

Accepted 8 January 2023

Available online 10 January 2023

Handling Editor: Z. Zhang

### Keywords:

Middle Jurassic

Mélange diapir melting

Crustal growth

Slab rollback

Central Tibet

## ABSTRACT

Andesitic rocks have similar compositions to average continental crust and have played a central role in improving our understanding of the formation and evolution of the continental crust. Here we present data for andesites from the Jiaqiong area of the Bangong–Nujiang suture zone (BNSZ), Central Tibet. LA-ICP-MS zircon U–Pb ages demonstrate that these andesites were generated during the Middle Jurassic (169–164 Ma). The Jiaqiong andesites have variable Mg<sup>#</sup> (molar  $100 \times \text{Mg}/[\text{Mg} + \text{Fe}] = 35\text{--}63$ ) values, and Cr (3.02–175 ppm) and Ni (5.70–47.7 ppm) contents. These andesitic rocks are enriched in light rare earth elements (REEs) ( $[\text{La}/\text{Yb}]_{\text{N}} = 5.2\text{--}14.6$ ) and yield relatively flat heavy REE patterns ( $[\text{Gd}/\text{Yb}]_{\text{N}} = 1.4\text{--}2.1$ ) with negative Ta, Nb, and Ti anomalies. They also have moderately high initial  $^{87}\text{Sr}/^{86}\text{Sr}$  (0.7077–0.7092) ratios and variable negative  $\varepsilon_{\text{Nd}}(\text{t})$  (−11.0 to −3.3) and zircon  $\varepsilon_{\text{Hf}}(\text{t})$  (−13.7 to +2.1) values. These geochemical characteristics suggest that the Jiaqiong andesites were most probably produced by partial melting of mélange rocks. Combining our data with the regional geology, particularly that of nearby ophiolites and Jurassic andesitic rocks, we conclude that the formation of these andesites was triggered by asthenospheric upwelling and hot corner flow caused by the rollback of the northward-subducting Bangong–Nujiang Tethyan oceanic lithospheric slab during the Middle Jurassic. The mélanges provided the material for the formation of andesites, and probably make a substantial contribution to the vertical growth of the continental crust in subduction zones.

© 2023 International Association for Gondwana Research. Published by Elsevier B.V. All rights reserved.

## 1. Introduction

The presence of continental crust is unique to Earth among the terrestrial planets (Hawkesworth and Kemp, 2006; Taylor and McLennan, 1985). The continental crust is geochemically similar to subduction-related andesitic rocks, suggesting that the growth of the continental crust is closely bound to subduction-related processes (Barth et al., 2000; Jagoutz et al., 2011; Kelemen and Behn, 2016; Taylor and McLennan 1985). Subduction zones are ideal sites for the formation and differentiation of continental crust (Moyen et al., 2017; Rudnick, 1995; Yogodzinski et al., 2010), where new continental crust can be produced through arc magmatism and

crustal material can be delivered to the deep mantle (Kelemen and Behn, 2016; Plank and Langmuir, 1993; Tatsumi and Hanyu, 2003; Tatsumi, 2005; Zheng and Zhao, 2017). Arc magmas have diverse compositions that reflect the complexity of their sources, which include oceanic sediments, altered oceanic crust, and the overlying mantle wedge (Hao et al., 2022; Jones et al., 2015; Marshall and Schumacher, 2012; Rocchi et al., 2015). Andesitic magmas that erupted above subduction zones at convergent plate boundaries are thought to have played an important role in the generation of the continental crust (Gómez-Tuena et al., 2014); however, the source of these andesitic magmas and details of the deep processes leading to their eruption are debated.

The Bangong–Nujiang suture zone (BNSZ) is located between the Lhasa and Qiangtang terranes in central Tibet and represents the remnants of the Bangong–Nujiang Tethyan Ocean (BNTO; Fig. 1a; Pan et al., 2012; Yin and Harrison, 2000; Zhang et al., 2012, 2014a; Zhu et al., 2016). The BNT oceanic lithospheric slab

\* Corresponding author at: State Key Laboratory of Isotope Geochemistry (SKLaBIG), Guangzhou Institute of Geochemistry (GIG), Chinese Academy of Sciences (CAS), Wushan Street, Guangzhou 510640, China.

E-mail address: [wqiang@gig.ac.cn](mailto:wqiang@gig.ac.cn) (Q. Wang).

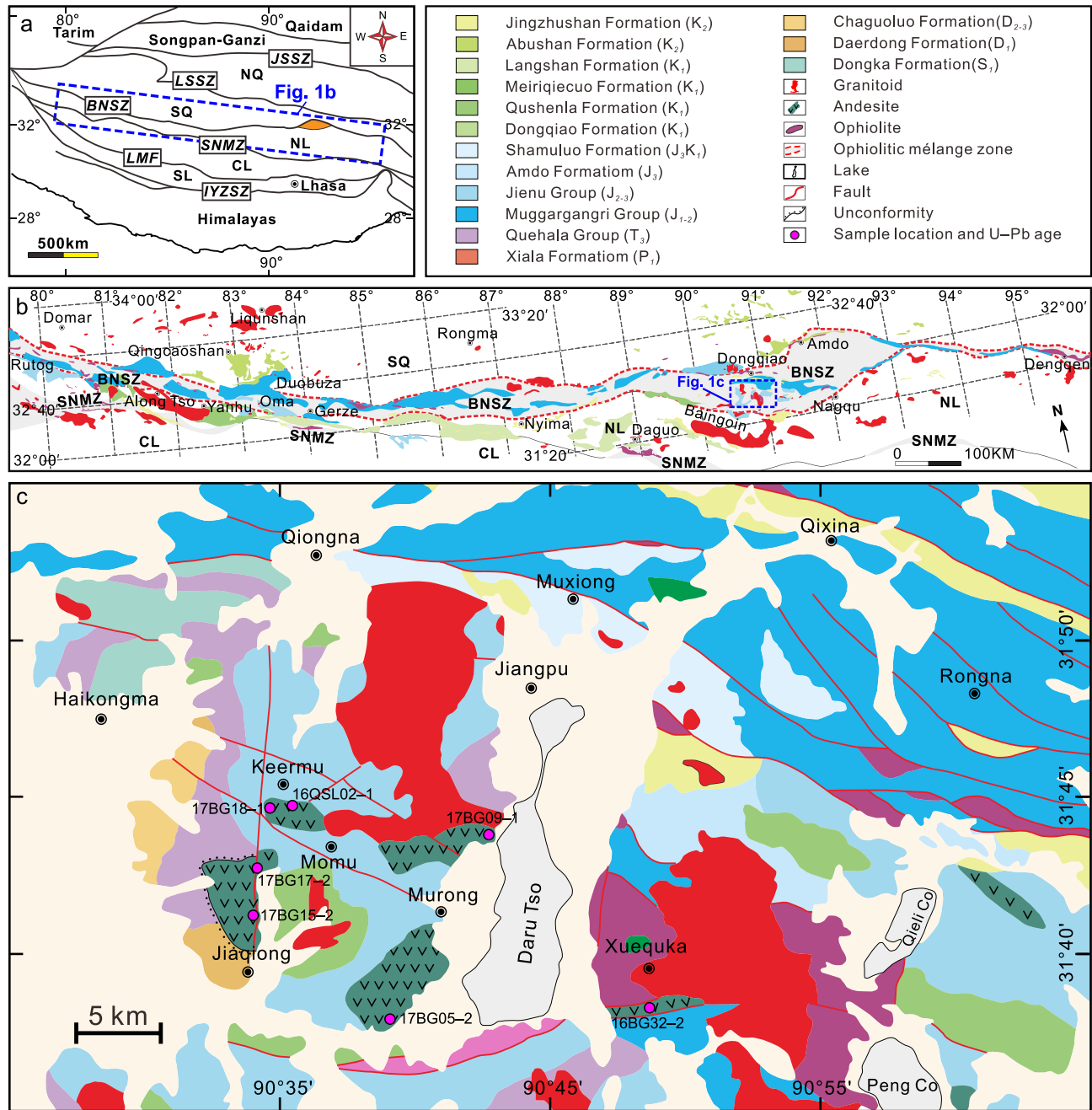


**Fig. 1.** (a) Sketch geological map of Tibet. (b) Geological map of the Bangong–Nujiang suture zone (modified after Zhu et al., 2016). (c) Geological map of the Jiaqiong area. JSSZ = Jinsha suture zone; NQ = Northern Qiangtang subterrane; LSSZ = Longmu Co–Shuanghu suture zone; SQ = Southern Qiangtang subterrane; BNSZ = Bangong–Nujiang suture zone; NL = Northern Lhasa subterrane; SNMZ = Shiquan River–Nam Tso mélange zone; CL = Central Lhasa subterrane; LMF = Luobadui–Milashan Fault; SL = Southern Lhasa subterrane; IYZSZ = Indus–Yarlung Zangbo suture zone.

was subducted beneath the southern Qiangtang subterrane, leading to intense arc magmatism along the BNSZ (Zhang et al., 2012; Zhu et al., 2016). Evidence of a continental arc along the southern margin of the southern Qiangtang subterrane includes the Jurassic magmatism in the Gerze area in the west (Li et al., 2014a, 2014b; Liu et al., 2014; Zhang et al., 2017c), the Kangqiong area in the middle segment (Li et al., 2016a; Yang et al., 2021b), and the Baigoin area (Zeng et al., 2016a; Tang et al., 2019) and Amdo terrane in the east part (Yan et al., 2016a). Owing to the subduction erosion and tectonic activity along the BNTO, large volumes of arc magmatic rocks have been destroyed and recycled into the deep mantle (Yang et al., 2021b). Fortunately, the Jurassic

andesitic rocks are well preserved in the middle–eastern parts of the southern Qiangtang margin (Fig. 1b, c). However, the petrogenesis and geodynamic processes of these andesitic rocks remain highly debated. Various geodynamic processes have been proposed to account for the generation of these andesitic rocks, including slab rollback (Yan et al., 2016a; Zhang et al., 2017b), intra-oceanic subduction (Tang et al., 2019; Yan and Zhang, 2020; Zhang et al., 2014a, 2021), and oceanic ridge subduction (Li et al., 2016a, 2020).

In this study, we report zircon U–Pb ages and Lu–Hf isotopes, mineral compositions, and whole-rock chemical and Sr–Nd isotopic compositions of andesites from the Jiaqiong area of the

middle–eastern parts of the BNSZ. Combining our results with data from previous studies of the andesitic rocks along the BNSZ, we discuss the petrogenesis and geodynamic processes of these rocks, shedding new light on the growth of continental crust and the evolution of continental arcs.

## 2. Geological setting and petrography

The Tibetan Plateau is located in the eastern part of the Tethyan Realm (Pan et al., 2012). It consists of four main continental terranes, from north to south: the Songpan–Ganzi, Qiangtang, Lhasa, and Himalaya, which are separated by the Jinsha suture zone (JSSZ), Bangong–Nujiang suture zone (BNSZ), and Indus–Yarlung Zangbo suture zone (IYZSZ), respectively (Fig. 1a; Pan et al., 2012; Yin and Harrison, 2000). The Qiangtang terrane is divided into the northern Qiangtang and southern Qiangtang subterrane by the Longmu Co–Shuanghu suture zone (LSSZ), which represents the remains of the main ocean basin of the Paleo-Tethyan Ocean (Fig. 1a; Fan et al., 2017; Zhai et al., 2016). The Lhasa terrane contains two major tectonic boundaries, the Shiquan River–Nam Tso Mélange zone (SNMZ) and the Luobadui–Milashan Fault (LMF), which subdivide this terrane into the northern, central, and southern Lhasa subterrane, respectively (Fig. 1a; Pan et al., 2012; Zhu et al., 2011, 2013). In central Tibet, the BNSZ marks the boundary between the southern Qiangtang subterrane to the north and the northern Lhasa subterrane to the south (Fig. 1b; Zhu et al., 2016), and consists of scattered ophiolitic fragments, radiolarian cherts, oceanic island (or seamount), arc volcanic-plutonic rocks, flysch-like deposits, and accretionary complexes (e.g., Fan et al., 2015, 2021; Wang et al., 2016; Zhang et al., 2021; Zhu et al., 2016). Some of ophiolitic fragments are considered as the remnants of BNT oceanic plateaus, corresponding to two major oceanic plateau eruptive events (i.e. 190–173 Ma and 128–104 Ma) within the BNTO (Yan and Zhang, 2020; Zhang et al., 2014a). The Early Jurassic oceanic plateau accreted to the southern Qiangtang margin and subsequently led to regional orogenesis, ocean-ward retreating, and intra-oceanic arc magmatism (Yan and Zhang, 2020; Zhang et al., 2021). The oceanic plateaus are represented by the Early Cretaceous Zhonggang ocean island (141–135 Ma; Fan et al., 2021).

The suture zone extends east–west for > 2000 km through the Bangong Co, Gerze, Dongqiao, Dengqen, and Jiayuqiao areas into Burma, Thailand, and Malaysia, and it can be subdivided into the western (Bangong Co–Gerze), the middle (Dongqiao–Amdo), and the eastern (Dengqen–Nujiang) segments (e.g., Pan et al., 2012; Yin and Harrison, 2000). In middle–eastern parts of the BNSZ, the main rock outcrops consist of Paleozoic sedimentary strata, Jurassic rock units (sandstones with interstratified volcanic rocks, flysch sediments, and limestones), Lower Cretaceous volcano-sedimentary units (volcanic rocks and conglomerates), granitoids, ophiolitic fragments and Quaternary deposits (Fig. 1c; Hu et al., 2017; Kapp and DeCelles, 2019; Wang et al., 2016; Zhang et al., 2014a). The Amdo terrane is an isolated microcontinent bounded by the Dongqiao–Amdo and Beila–Lanong ophiolite belts (Zhu et al., 2011), and consists mainly of strongly foliated gneisses, metasedimentary rocks, and undeformed granitoids (Guynn et al., 2006, 2012; Zhang et al., 2014b; Zhu et al., 2013). Previous studies have shown that the ophiolitic fragments in the Baingoin and Amdo areas were produced during the Early Jurassic (ca. 188 Ma; Liu et al., 2016) and Late Jurassic (ca. 148 Ma; Zhong et al., 2017), and formed in a fore-arc oceanic setting (Wang et al., 2016). The Early Cretaceous strata (Duoni and Duoba Formations) were widely deposited in middle–eastern segments of the BNSZ, and their provenance data, specifically detrital zircon U–Pb age spectra, indicate that the collision of Lhasa–Qiangtang terrane

took place during late Early Cretaceous (122–113 Ma; Lai et al., 2019; Zhu et al., 2019). Therefore, the BNTO was not closed between 148 and 122 Ma, which is consistent with the results from the remnants of oceanic plateau within the BNSZ (Yan and Zhang, 2020; Zhang et al., 2014a). The volcanic rocks from the Baingoin–Amdo areas can be divided into two major stages: the Jurassic (185–150 Ma) and the Early Cretaceous (126–100 Ma). The Early Cretaceous volcanic rocks unconformably overlie the Jurassic rock units and are exposed widely in the BNSZ and the northern part of the Lhasa terrane (e.g., the Qushenla and Duoni Formations, Hu et al., 2017; Zhu et al., 2016). These rocks are interpreted to have been derived from the Lhasa–Qiangtang collision (Hu et al., 2017; Qu et al., 2012) or the Andean-style orogenic collapse related to the subduction of the NeoTethyan Ocean (Zhang et al., 2012). Although the Middle–Late Jurassic arc volcanic rocks are less distributed than the Early Cretaceous volcanic rocks within the BNSZ (Tang et al., 2019; Yang et al., 2021b; Zeng et al., 2016a), these rocks have important implications for tectonic evolution of the BNTO.

Andesite samples investigated in this study were collected from the Jiaqiong area in the middle–eastern segments of the BNSZ. These andesites unconformably overlie the Early Devonian and Late Triassic strata, and are in fault contact with the Jiang Co ophiolites and the Muggargangri Group, according to field observations (Fig. 1c). The rocks are porphyritic with grayish-green to grayish-black color (Fig. 2a, b), and contain euhedral–subhedral feldspar (~10 vol%), biotite (~1 vol%) and subhedral–xenomorphic clinopyroxene (~5 vol%) phenocrysts (Fig. 2c, d). The groundmass in the andesitic rocks is composed primarily of feldspar and clinopyroxene microlites and altered glass. Epidote and chlorite are secondary minerals, and accessory minerals include zircon, apatite, titanite, and Fe–Ti oxides.

## 3. Analytical methods and results

LA-ICP-MS zircon U–Pb dating was conducted at the Institute of Geology and Geophysics, Chinese Academy of Sciences (IGG CAS). Whole-rock major- and trace-element and Sr–Nd isotope, mineral chemistry, and zircon Hf isotopic analyses were carried out at the State Key Laboratory of Isotope Geochemistry, Guangzhou Institute of Geochemistry, Chinese Academy of Sciences (SKLa-BIG GIG CAS). Details of the analytical procedures and results are presented in the Supplemental Material.

### 3.1. Zircon U–Pb ages

Seven samples of andesite from the Jiaqiong area were selected for zircon U–Pb dating (16BG32–2, 16QSL02–1, 17BG05–2, 17BG09–1, 17BG15–2, 17BG17–2, and 17BG18–1). Most zircon grains from the seven samples are transparent and colorless under an optical microscope, and they are 100–300 µm in length with length/width ratios of 1:1 to 3:1. Most of the zircon grains show concentric oscillatory zoning in cathodoluminescence (CL) images (Fig. 3), and yield high and variable Th (39–6391 ppm) and U (85–2118 ppm) contents with Th/U ratios of 0.45–4.89, indicating a magmatic origin (Hoskin and Schaltegger, 2003). U–Pb concordia diagrams for the analyzed zircon grains are shown in Fig. 3, and the U–Pb age data are presented in Table S1.

The studied samples (16BG32–2, 16QSL02–1, 17BG05–2, 17BG09–1, 17BG15–2, 17BG17–2, and 17BG18–1) yield weighted mean  $^{206}\text{Pb}/^{238}\text{U}$  ages of  $169.2 \pm 1.2$  Ma,  $166.1 \pm 0.8$  Ma,  $166.9 \pm 1.6$  Ma,  $167.0 \pm 1.2$  Ma,  $164.2 \pm 1.5$  Ma,  $168.4 \pm 2.1$  Ma, and  $166.3 \pm 1.6$  Ma, respectively (Fig. 3), suggesting that the Jiaqiong volcanic rocks were erupted between 169 and 164 Ma.

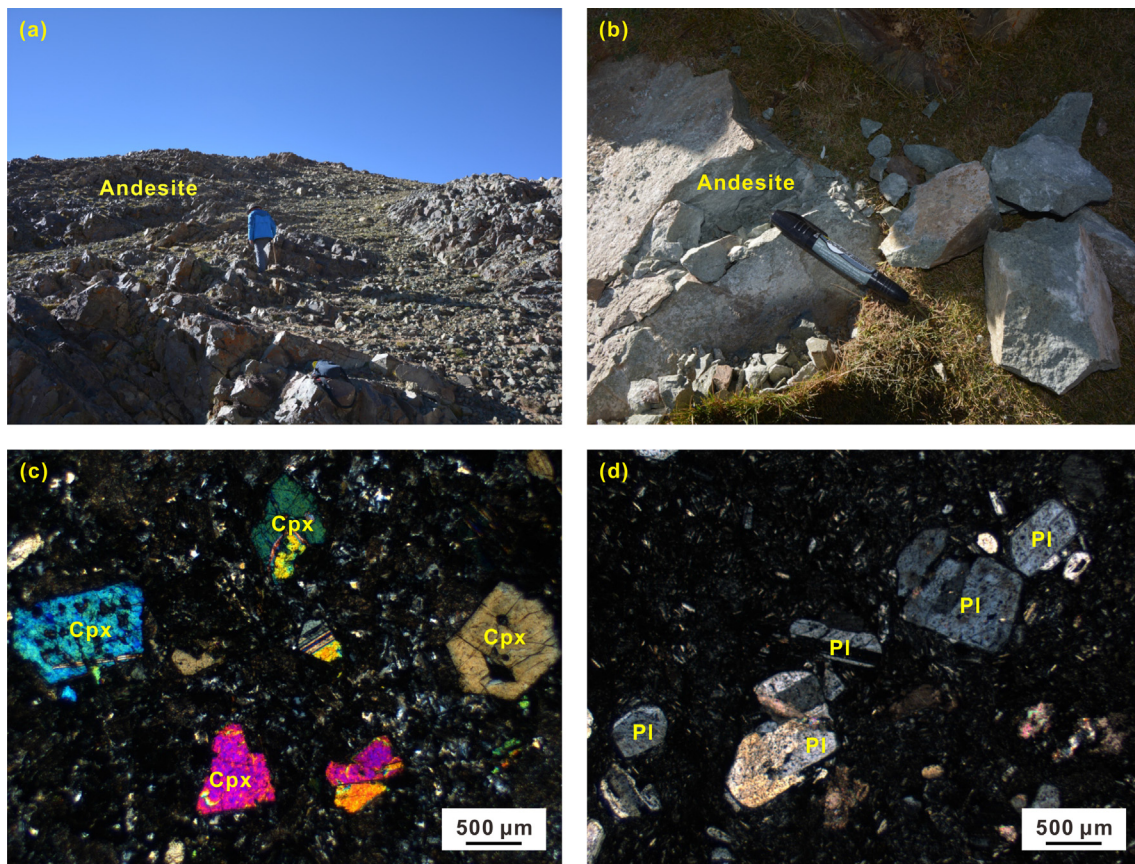


**Fig. 2.** (a–b) Representative field photographs and (c–d) photomicrographs illustrating the petrographic characteristics of the Jiaqiong andesites. Mineral abbreviations: Cpx = clinopyroxene; Pl = plagioclase.

### 3.2. Mineral chemistry

The clinopyroxene (Cpx) crystals in the Jiaqiong andesites are mostly augite with variable compositions ( $\text{Wo}_{37.3\text{--}42.7}\text{En}_{41.2\text{--}45.4}\text{Fs}_{13.5\text{--}20.7}$ ; Table S2; Fig. 4). They have low  $\text{Al}_2\text{O}_3$  (1.85–3.53 wt%),  $\text{TiO}_2$  (0.29–0.85 wt%) and  $\text{Na}_2\text{O}$  (0.21–0.46 wt%) contents, and high  $\text{Mg}^{\#}$  (67.0–76.4) values. The Cpx phenocrysts are subhedral to euhedral and show oscillatory zoning (Fig. 5).

### 3.3. Effects of alteration

Petrographical observations and loss on ignition (LOI = 2.39–5.27 wt%) values suggest that the Jiaqiong andesite samples probably have experienced varying degrees of alteration. In general, zirconium (Zr) is the most immobile element in low-grade metamorphism and alteration process (e.g., Gibson et al., 1982; Wood et al., 1979). Therefore, correlations between Zr and other elements can be used to discriminate the mobility of elements during post-magmatic processes (Polat and Hofmann, 2003). The large ion lithophile elements (LILEs; e.g., K, Rb, and Ba) of the Jiaqiong andesites show no obvious variation with Zr (Fig. 6a, b), indicating that they have probably been modified by alteration. The high field strength elements (HFSEs; e.g., Nb, Ta, P, and Hf; Fig. 6c–f), rare earth elements (REEs), and Y (Fig. 6g, h) are strongly correlated with Zr, suggesting that these elements were essentially immobile during alteration. On a diagram of Zr versus initial  $^{87}\text{Sr}/^{86}\text{Sr}$  isotopic ratios [ $(^{87}\text{Sr}/^{86}\text{Sr})_i$ ] (Fig. 6i), the  $(^{87}\text{Sr}/^{86}\text{Sr})_i$  ratios are positively correlated with Zr, implying that the  $(^{87}\text{Sr}/^{86}\text{Sr})_i$  ratios of the Jiaqiong andesites probably represent the original isotopic signatures. Thus, immobile elements such as  $\text{MgO}$ ,  $\text{TiO}_2$ ,  $\text{P}_2\text{O}_5$ , HFSEs,

REEs, transitional elements (e.g., Cr and Ni), and Sr–Nd isotope compositions are mainly used in following discussion.

### 3.4. Whole-rock major and trace element compositions

Major and trace element data for the studied andesite samples are listed in Table S3. The Jiaqiong andesites have variable  $\text{SiO}_2$  (52.0–65.9 wt%) and  $\text{MgO}$  (1.51–4.66 wt%) contents with moderate  $\text{Mg}^{\#}$  (35–63) values, and low  $\text{TiO}_2$  (0.53–0.87 wt%), Cr (3.02–175 ppm), and Ni (5.70–47.7 ppm) contents. On the  $\text{Zr}/\text{TiO}_2$  versus  $\text{Nb}/\text{Y}$  diagram of Winchester and Floyd (1977), the Jiaqiong andesite samples plot in the field for andesitic rocks, with  $\text{Nb}/\text{Y}$  ratios of 0.23–0.89 (Fig. 7a). On a Th versus Co classification diagram for altered volcanic rocks (Hastie et al., 2007), the Jiaqiong andesites plot in the high-K calc-alkaline field (Fig. 7b). These rocks have relatively low and variable total REE contents (84–196 ppm) and are characterized by moderate enrichment in light REEs (LREEs), relatively flat heavy REE (HREE) patterns ( $[\text{La}/\text{Yb}]_N = 5.15\text{--}14.59$ ), and moderate negative Eu anomalies ( $\text{Eu}/\text{Eu}^* = \text{Eu}_N/\sqrt{\text{Sm}_N \times \text{Gd}_N} = 0.65\text{--}0.89$ ; Fig. 8a). On a primitive mantle-normalized spider diagram, the andesites are slightly enriched in some incompatible elements (e.g., Th and U) and strongly depleted in Nb, Ta, Ti, and P (Fig. 8b).

### 3.5. Whole-rock Sr–Nd isotopic compositions

Whole-rock Sr–Nd isotopic data for the Jiaqiong andesites are listed in Table S4 and shown in Fig. 9a. Zircon U–Pb weighted mean ages from this study were used to calculate the initial Sr–Nd isotopic compositions. The Jiaqiong andesites yield high initial

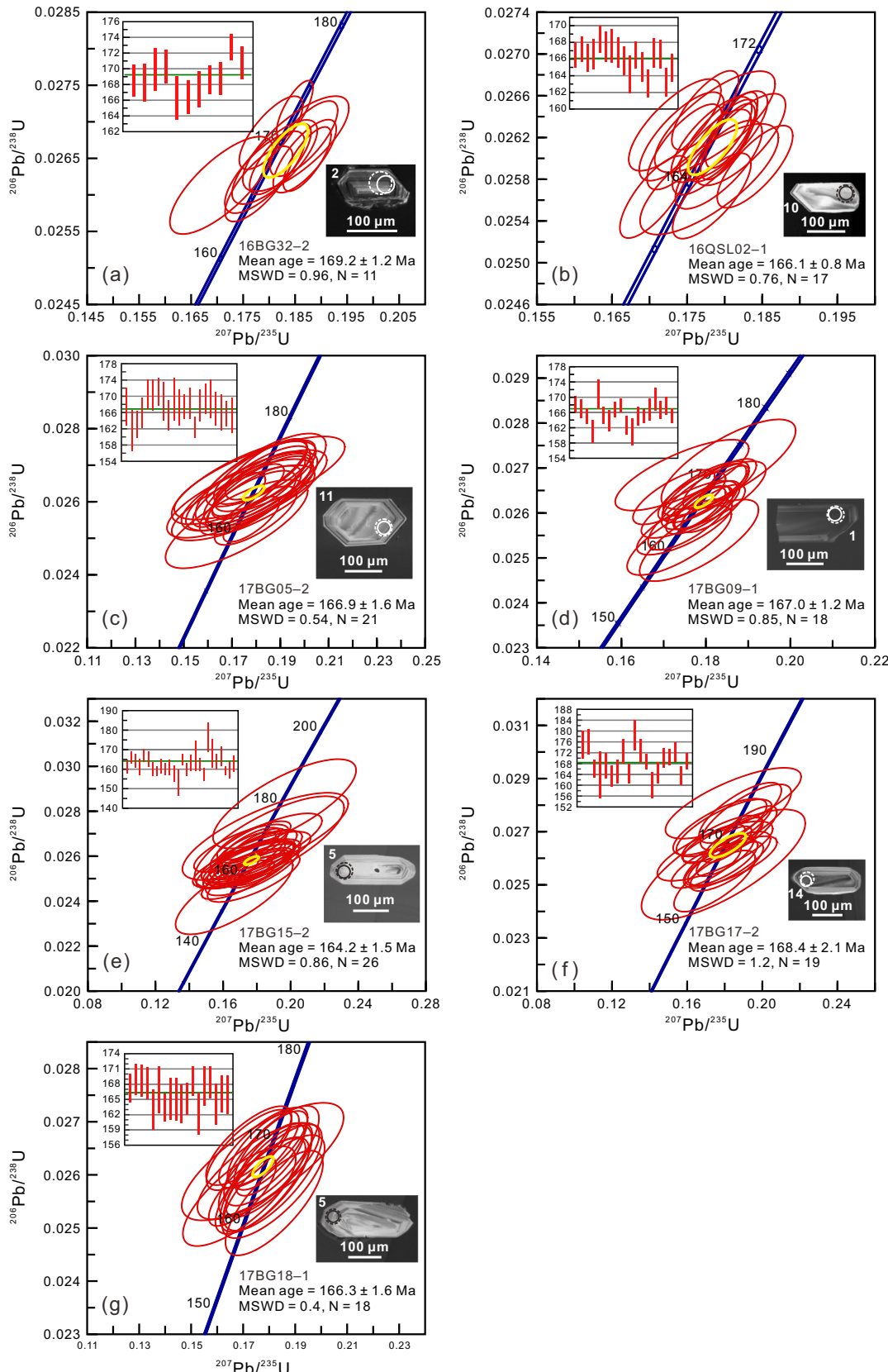


**Fig. 3.** Representative cathodoluminescence (CL) images and U-Pb concordia plots for zircon grains from the Jiaqiong andesites. Solid and dashed circles indicate the locations of U-Pb age and *in situ* Hf isotopic analyses, respectively.

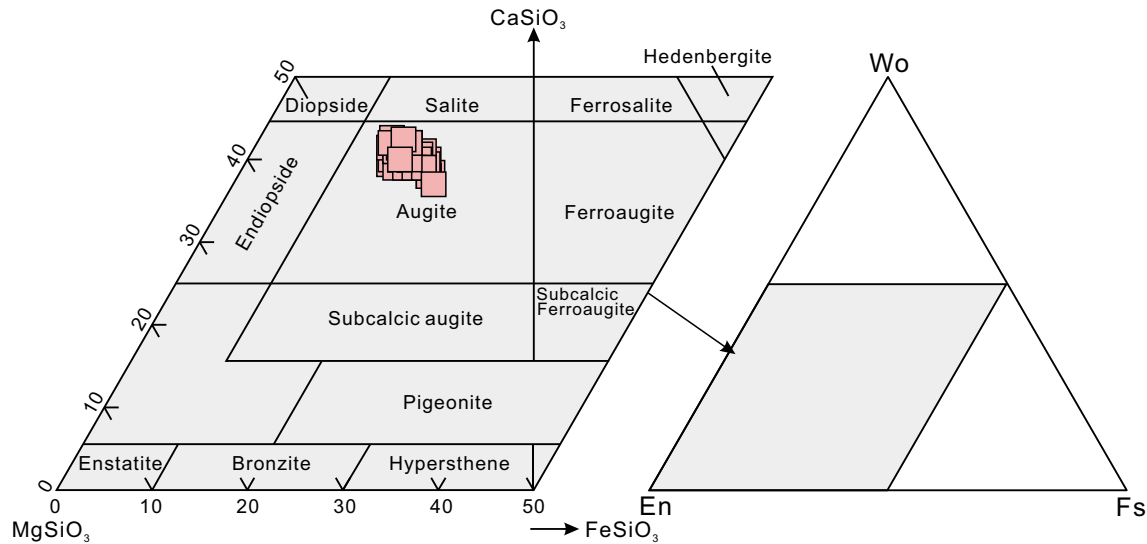


**Fig. 4.** CaSiO<sub>3</sub>-MgSiO<sub>3</sub>-FeSiO<sub>3</sub> diagram (Morimoto, 1988) showing the compositions of pyroxene phenocrysts from the Jiaqiong andesites.

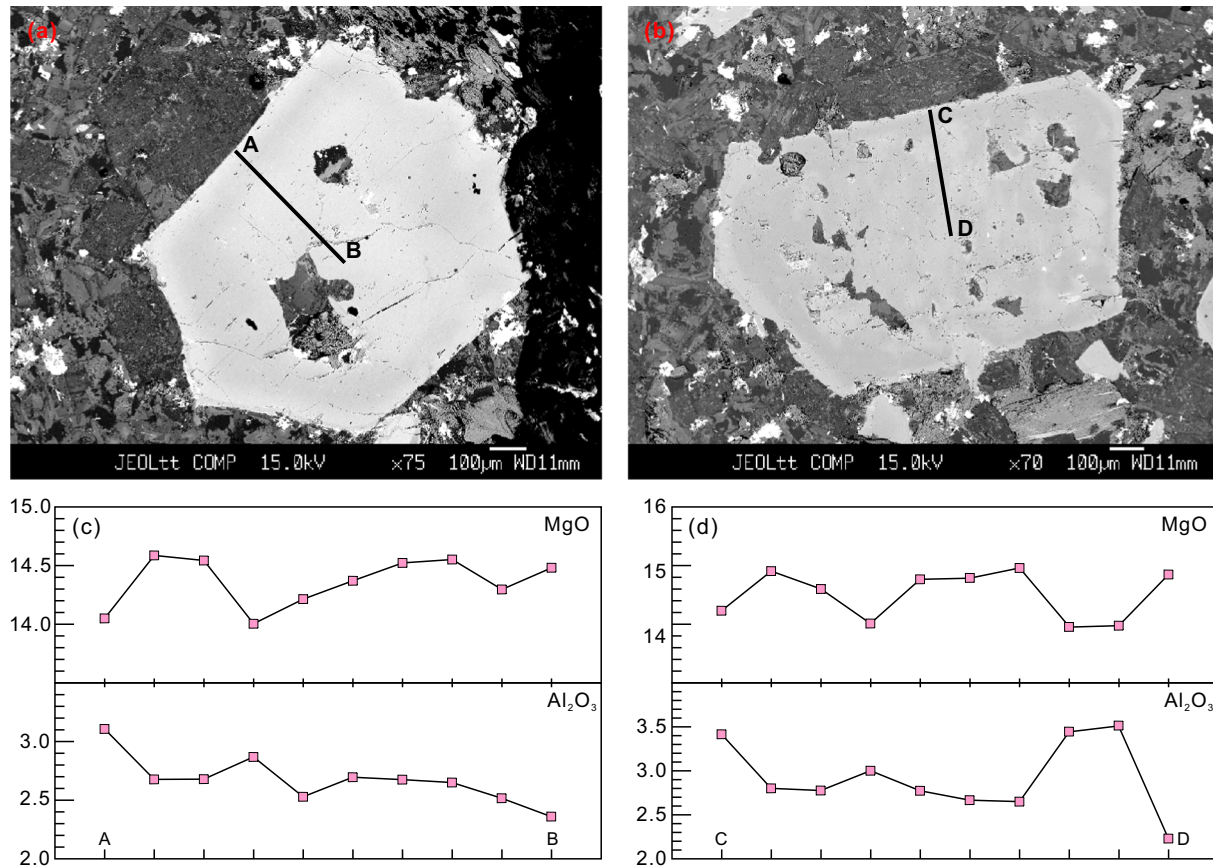


**Fig. 5.** (a–b) Representative back-scattered electron (BSE) images and (c–d) corresponding compositional traverses across clinopyroxene phenocrysts from the Jiaqiong andesites.

$^{87}\text{Sr}/^{86}\text{Sr}$  ratios (0.7077–0.7092), and negative and variable  $\varepsilon_{\text{Nd}}(\text{t})$  (−11.0 to −3.3) values, with single-stage Nd model ages ( $T_{\text{Nd}}^{\text{DM}}$ ) ranging from 1.73 to 1.28 Ga (Fig. 9a and Table S4). The Sr-Nd isotopic compositions of the Jiaqiong andesites are similar to those of the Darutso high-magnesium andesitic rocks (Zeng et al., 2016a) but differ from those of the Dongqiao Jurassic ophiolites, which have lower initial  $^{87}\text{Sr}/^{86}\text{Sr}$  ratios and higher  $\varepsilon_{\text{Nd}}(\text{t})$  values (Fig. 9a; Liu et al., 2016; Wang et al., 2016).

### 3.6. Zircon Lu-Hf isotopic compositions

*In situ* LA-MC-ICP-MS Lu-Hf isotope analyses were conducted on zircon grains that had been used in dating analyses. Zircon Hf isotopic data are presented in Table S5. Zircon grains from the Jiaqiong andesites yield variable initial  $^{176}\text{Hf}/^{177}\text{Hf}$  values (0.282286–0.282726) and negative to positive  $\varepsilon_{\text{Hf}}(\text{t})$  values (−13.7 to +2.1; Fig. 9b).

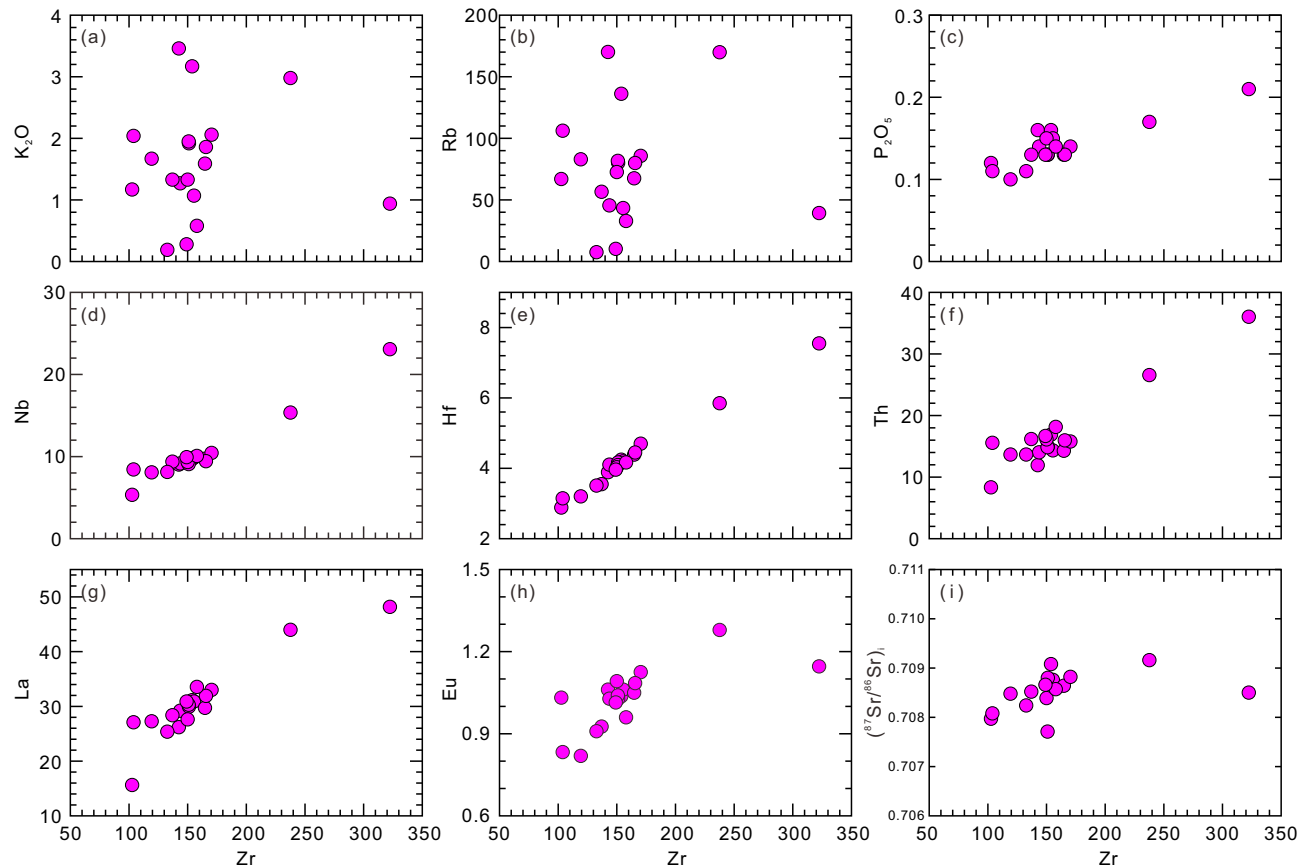


**Fig. 6.** Whole-rock major- and trace-element contents and  $(^{87}\text{Sr}/^{86}\text{Sr})_i$  ratios plotted against Zr contents for the Jiaqiong andesites.

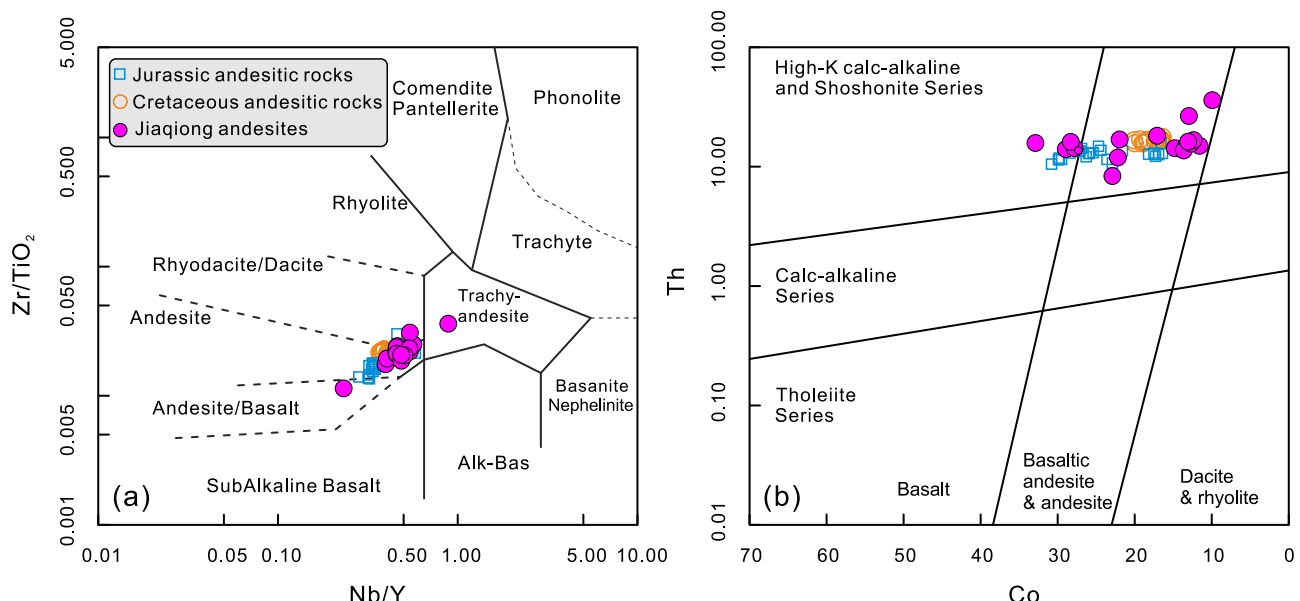


**Fig. 7.** (a)  $\text{Zr}/\text{TiO}_2$  versus  $\text{Nb}/\text{Y}$  (Winchester and Floyd, 1977) and (b) Th versus Co (Hastie et al., 2007) diagrams. Data for the Jurassic and Cretaceous andesitic rocks are from Tang et al. (2019) and Hu et al. (2017), respectively.

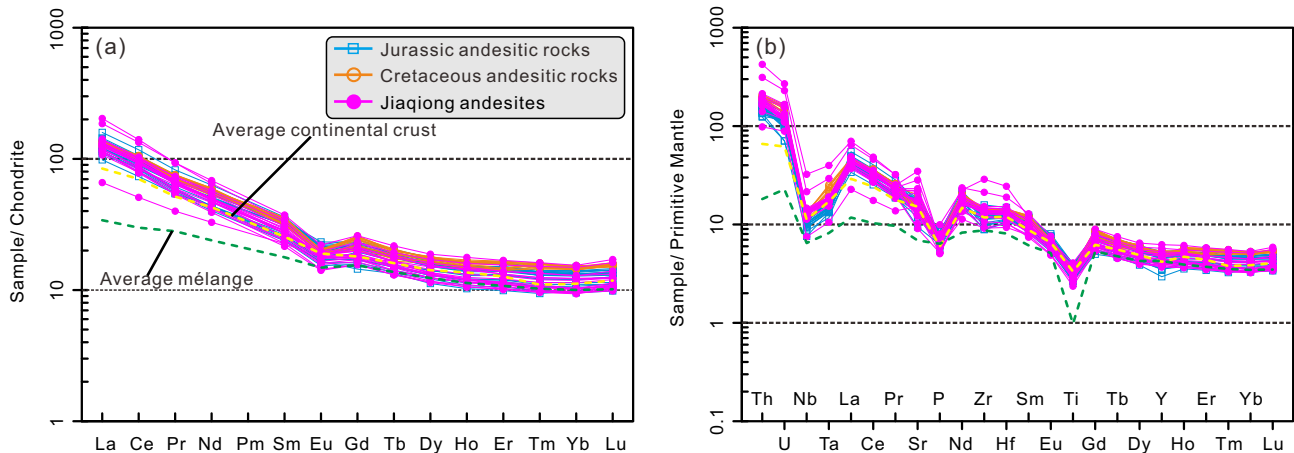


**Fig. 8.** (a) Chondrite-normalized REE patterns and (b) primitive mantle-normalized trace element spider diagrams for the Jiaqiong andesites. Normalization values are from Sun and McDonough (1989). The average mélange composition (dashed green line) is from Marschall and Schumacher (2012) and the average continental crust composition (dashed yellow line) is from Rudnick and Gao (2003).

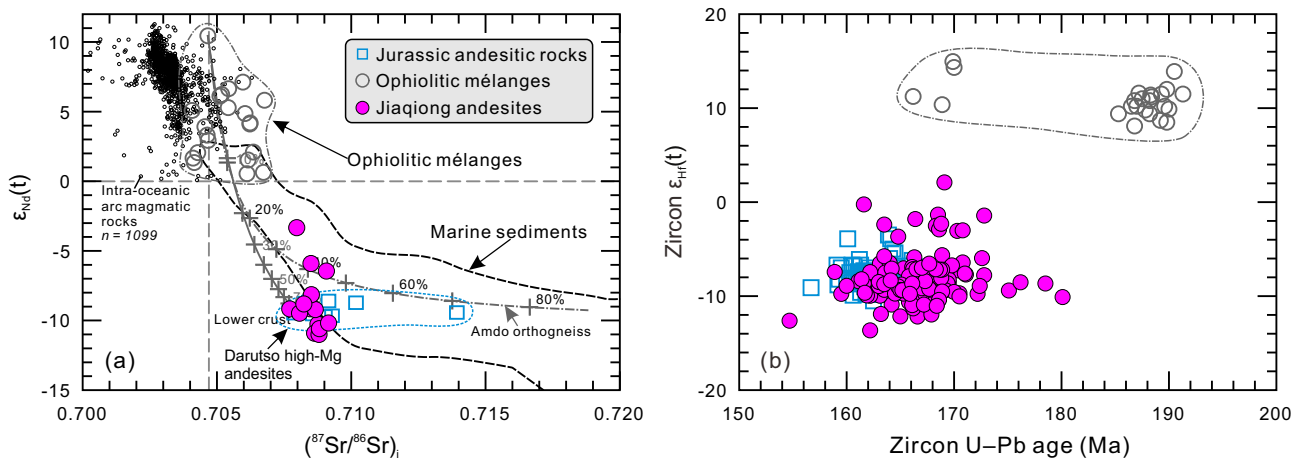


**Fig. 9.** (a)  $\epsilon_{\text{Nd}}(t)$  versus  $(^{87}\text{Sr}/^{86}\text{Sr})$ , and (b) zircon  $\epsilon_{\text{Hf}}(t)$  versus U-Pb age diagrams. Data for ophiolitic mélanges are from Huang et al. (2015), Liu et al. (2016) and Yang et al. (2019), and data for Jurassic andesitic rocks are from Tang et al. (2019), Yan et al. (2016a), and Zeng et al. (2016a, 2016b). Upper and lower crustal Sr-Nd isotopic compositions are from Harris et al. (1988) and Hu et al. (2020), respectively. Data for intra-oceanic arc magmatic rocks are from GEOROC (<http://georoc.mpch-mainz.gwdg.de/georoc/>).

## 4. Discussion

### 4.1. Tectonic setting

Previous studies have proposed that the BNTO was present until the Late Cretaceous (Cao et al., 2019; Fan et al., 2015, 2021; Hao et al., 2019; Kapp and DeCelles, 2019; Zhang et al., 2012, 2014a, 2017a, 2017c; Zeng et al., 2016a; Zhu et al., 2016) and that its closure was diachronous (Fan et al., 2018; Hu et al., 2022; Yan et al., 2016b). In the middle-eastern parts of the BNSZ, zircon U-Pb ages of ophiolites indicate that the BNTO was not closed during the Late Jurassic (ca. 148 Ma) (Liu et al., 2016; Zhong et al., 2017). Voluminous Middle-Late Jurassic magmatic rocks are exposed along the southern margin of the southern Qiangtang subterrane, and these rocks are thought to have been generated by subduction of the BNT oceanic lithosphere (Hu et al., 2020; Li et al., 2014a, 2014b; Liu et al., 2017; Tang et al., 2019; Zhang et al., 2012, 2017b; Zeng et al., 2016a). Paleomagnetic data from the Middle Jurassic limestones in the southern Qiangtang subterrane indicate that the BNTO was still open at that time (Cao et al., 2019). Therefore, all results suggest an oceanic subduction tectonic setting for the middle-eastern parts of the BNSZ during the Jurassic.

### 4.2. Magmatic evolution

#### 4.2.1. Crustal assimilation

Volcanic rocks are generally susceptible to contamination during their ascent through the continental crust or when they erupt on the Earth's surface (e.g., Castillo et al., 1999; Depaolo, 1981). Thus, the effects of crustal contamination need to be evaluated before investigating the petrogenesis of the Jiaqiong andesites. Crustal contamination usually produces strong linear relationships between fractionation indices (e.g., SiO<sub>2</sub>, MgO, Nb/La, and Sm/Nd) and isotopic compositions (e.g., Sr-Nd isotopic compositions) owing to the large compositional differences between mantle and crustal materials. The Jiaqiong andesites show no such correlations (Fig. 10a-d), indicating that crustal contamination has played a minor role in the formation of these rocks. This is also supported by the absence of inherited zircon grains in the Jiaqiong andesites (Table S1). Moreover, Sr-Nd mixing models suggest that the assimilation of 30–70 % of the southern Qiangtang lower crust or 30–50 % upper crustal material would have been required to produce the isotopic compositions of the Jiaqiong andesites (Fig. 9a); however, such a high proportion of crustal materials would produce felsic rocks rather than intermediate rocks. Therefore, we suggest

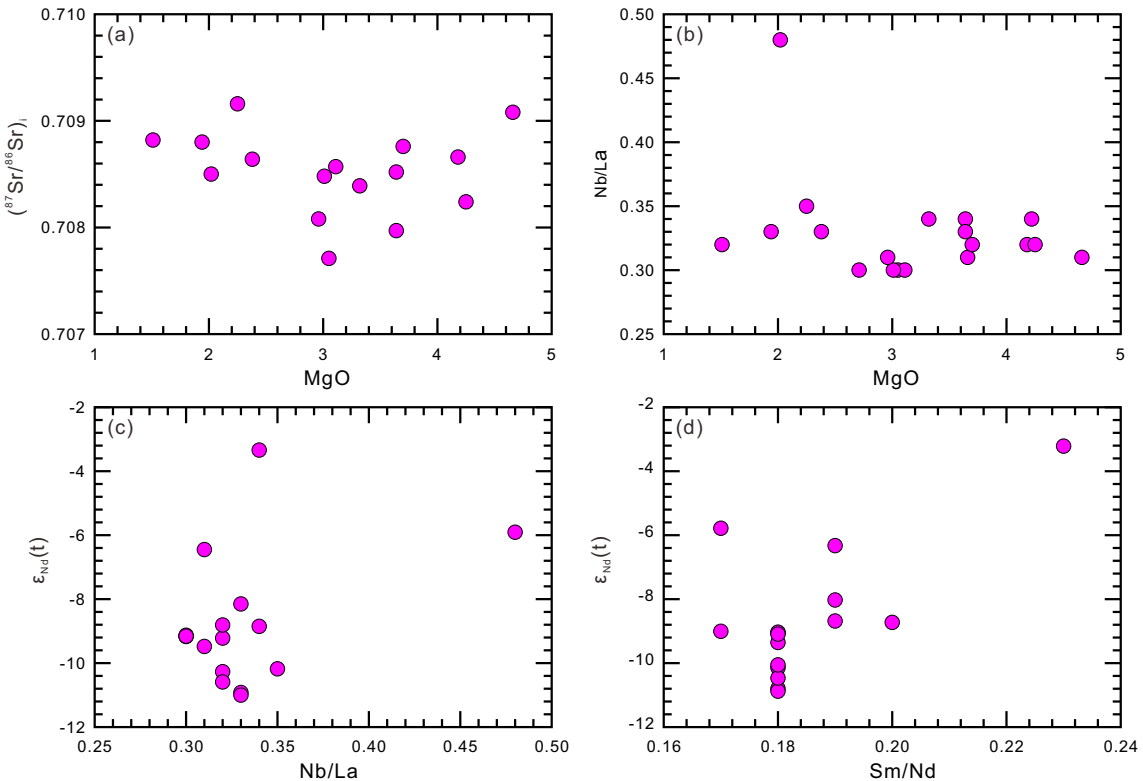


**Fig. 10.** Plots of (a)  $(^{87}\text{Sr}/^{86}\text{Sr})_i$  versus MgO, (b) Nb/La versus MgO, (c)  $\epsilon_{\text{Nd}}(t)$  versus Nb/La, and  $\epsilon_{\text{Nd}}(t)$  versus Sm/Nd for the Jiaqiong andesites.

that crustal contamination played a negligible role in the formation of the Jiaqiong andesites during the magma ascent and emplacement.

#### 4.2.2. Fractional crystallization versus partial melting

The Jiaqiong andesites yield lower and more variable Mg<sup>#</sup> (35–63) values and Cr (3.02–175 ppm) and Ni (5.70–47.7 ppm) contents than primary mantle-derived magmas ( $\text{Mg}^{\#} > 70$ , Cr > 1000 ppm, Ni > 400–500 ppm; Wilson, 2007). However, fractional crystallization for these rocks can be ruled out given that: (1) fractional crystallization of basaltic magmas can indeed produce more evolved magmas (Zheng et al., 2015), but it is unlikely to generate large amounts of the Jiaqiong andesites due to the absence of coeval basaltic rocks in study area; (2) the Jiaqiong andesite samples plot along the trend of partial melting rather than fractional crystallization trends on La versus La/Sm and La versus La/Yb diagrams (Fig. 11a, b); and (3) some elements have large ranges at certain SiO<sub>2</sub> contents or Mg<sup>#</sup> values, indicating that the primary melts have highly heterogeneous major-element compositions (Table S3). We conclude, therefore, that the Jiaqiong andesites were generated mainly by partial melting and that their heterogeneous geochemical compositions were inherited from their magma sources.

#### 4.3. Petrogenesis of the Jiaqiong andesites

Andesitic rocks may be generated by several processes, including (1) partial melting of mafic lower crust (e.g., Cai et al., 2015; Jung et al., 2002; Petford and Atherton, 1996); (2) mixing between mantle-derived basaltic and crust-derived felsic magmas (e.g., Reubi and Blundy, 2009; Straub et al., 2011; Streck et al., 2007); (3) fractional crystallization of basaltic magmas (e.g., Lee and Bachmann, 2014; Pichavant and Macdonald, 2007; Stevenson et al., 1999); (4) partial melting of mantle wedge that had been

metasomatized by slab-derived melts or fluids (e.g., Grove et al., 2002; Mitchell and Grove, 2015; Shimoda et al., 1998); and (5) partial melting of subducted mélange (e.g., Codillo et al., 2018; Cruz-Uribe et al., 2018; Hao et al., 2016, 2022; Marschall and Schumacher, 2012; Nielsen and Marschall, 2017). The large range of isotope compositions of the Jiaqiong andesites can be attributed to either a heterogeneous source region or magma mixing between basaltic and felsic melts. The majority of Jiaqiong andesite samples show lower  $\epsilon_{\text{Nd}}(t)$  values than crustal compositions of the study area and are not distributed along Sr-Nd isotope mixing curves (Fig. 9a), ruling out the possibility of significant magma mixing. The absence of mafic microgranular enclaves (MMEs) in these andesites also indicates that magma mixing is not considered as a plausible mechanism accounting for their formation (e.g., Farner et al., 2014). Thus heterogeneous geochemical compositions of the Jiaqiong andesites were inherited from their magma sources. Experimental studies have shown that dehydration melting of basaltic and pelitic crustal rocks produces low-Mg<sup>#</sup> (generally < 40) melts regardless of the degree of melting (e.g., Rapp and Watson, 1995). The Jiaqiong andesites have high and variable Mg<sup>#</sup> values (43–63, except for one sample with a Mg<sup>#</sup> of 35), indicating they were derived mainly from the mantle rather than the crustal material. The Jiaqiong andesites have lower MgO and compatible trace element contents (e.g., Cr and Ni), and more enriched Sr-Nd-Hf isotopic compositions than mid-ocean ridge basalts (MORB) from the Bangong–Nuijiang Tethyan ophiolites (Fig. 9; Liu et al., 2016; Wang et al., 2016; Zhong et al., 2017). These andesitic rocks are also characterized by relative enrichment in LILEs, LREEs and U, and depletion in HFSEs (e.g., Nb, Ta, Ti, and P) in the primitive mantle-normalized spider diagrams, indicating a typical arc-like geochemical affinity (Fig. 8b). Therefore, the subducted oceanic slab components were probably added to the sub-arc mantle in the forms of aqueous fluids, sediment-derived melts, or bulk sediment (Class et al., 2000). Aqueous fluids carry very limited REEs,

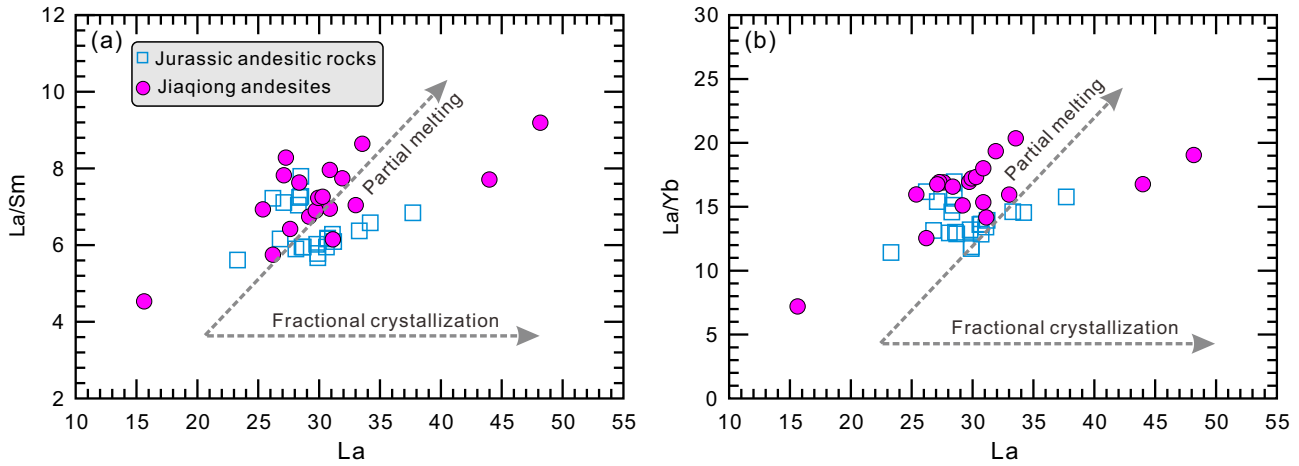


**Fig. 11.** (a) La/Sm versus La and (b) La/Yb versus La diagrams for the Jiaqiong andesites. Data for the Jurassic andesitic rocks are from Tang et al. (2019).

Th, and HFSEs (e.g., Hf, Nb, Zr, and Ta) but considerable amounts of LILEs (e.g., K, Rb, Ba, and Sr) and other fluid-mobile trace elements (e.g., U and Pb; e.g., Guo et al., 2013). The Jiaqiong andesites have significantly higher Th/Nb, Th/Nd and Th/La ratios (Fig. 12a–c) than oceanic basalts from the Bangong–Nujiang Tethyan ophiolite suites (Liu et al., 2016; Zhong et al., 2017), indicating that slab-derived fluids did not make a dominant contribution to their magma sources. On a plot of U/Th versus Th/Nb (Fig. 12a), the Jiaqiong andesites did not show an enriched tendency of aqueous fluids or melts, further suggesting the insignificant contribution of aque-

ous fluids or sediment-derived melts to magmatic sources. The initial Sr–Nd isotopic compositions of the Jiaqiong andesite samples plot along the mixing line between those of the subducted bulk sediments and oceanic basalts (Fig. 12d), indicating that bulk oceanic sediment was probably added to their magma sources. Therefore, we suggest that bulk sediment—rather than aqueous fluids or sediment melts—was most probably incorporated into the source of the Jiaqiong andesites.

The Jiaqiong andesites were not substantially affected by crustal contamination (Fig. 10), and their geochemical and isotopic sig-

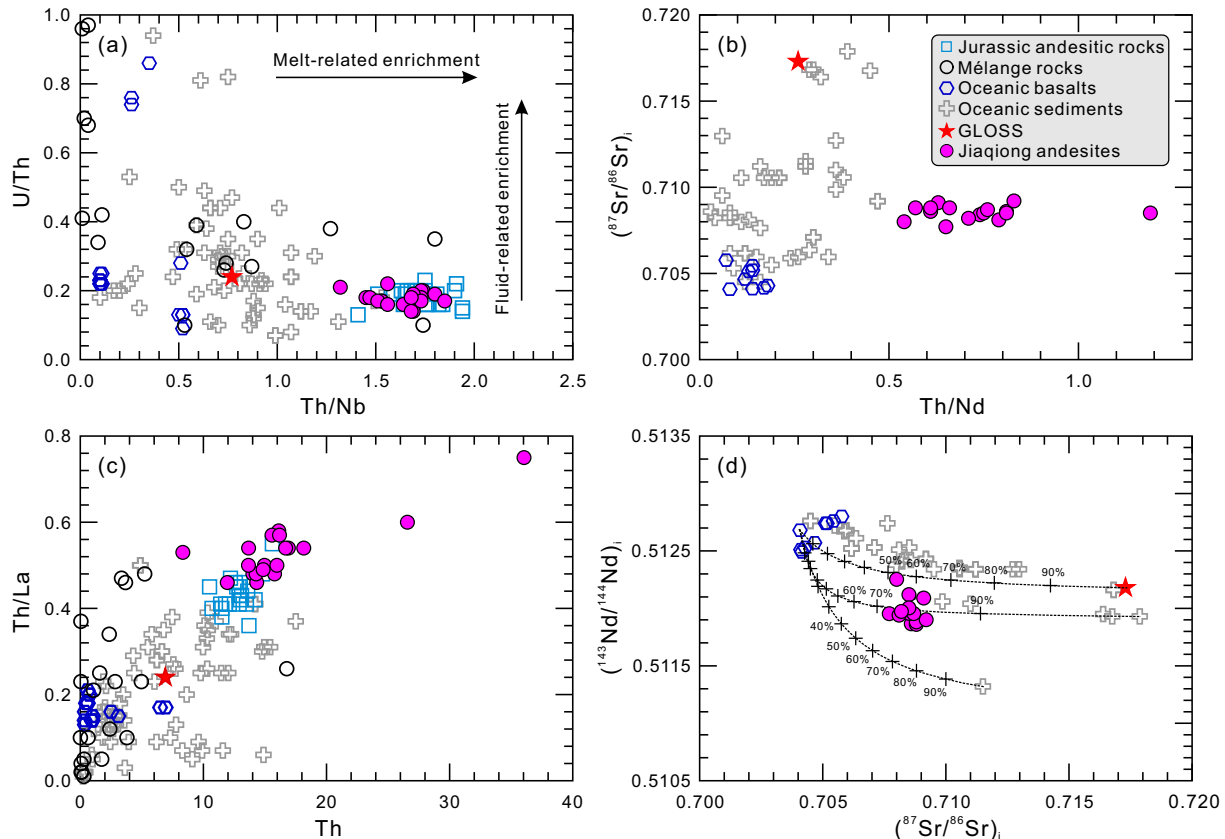


**Fig. 12.** (a) U/Th versus Th/Nb, (b)  $(^{87}\text{Sr}/^{86}\text{Sr})_i$  versus Th/Nd, (c) Th/La versus Th, and (d)  $(^{143}\text{Nd}/^{144}\text{Nd})_i$  versus  $(^{87}\text{Sr}/^{86}\text{Sr})_i$  diagrams. Data for the Jurassic andesitic rocks are from Tang et al. (2019), those for oceanic sediment and GLOSS (global subducting sediment) are from Plank and Langmuir (1998), and those for oceanic basalts in ophiolites are from Liu et al. (2016) and Zhong et al. (2017).

tures were mainly inherited from source region. These andesites show variable MgO (1.51–4.66 wt%) contents and  $\varepsilon_{\text{Nd}}(t)$  (−11.0 to −3.3) values, indicating that these rocks were derived from a heterogeneous magma source. This interpretation is further corroborated by the oscillatory zoning in the Cpx phenocrysts from the Jiaqiong andesites (Fig. 5). Mélange rocks are formed by the physical mixing of subducted sediments, oceanic crust, and peridotite mantle rocks along the slab-mantle interface (e.g., Cruz-Uribe et al., 2018; Marschall and Schumacher, 2012). These mixed material transfer into the mantle wedge via diapirs that rise buoyantly from the slab surface, producing arc magmas with diverse geochemical signatures (e.g., Codillo et al., 2018; Hao et al., 2022; Nielsen and Marschall, 2017). The range of compositions of the Jiaqiong andesites may reflect the characteristics of arc magmas that derived from mélanges (Fig. 12b–d). The Jiaqiong andesitic rocks are enriched in LILEs and LREEs, and depleted in HFSEs, similar to those of the mélange rocks (Fig. 8b). In addition, the Jiaqiong andesites show relatively heterogeneous isotopic compositions (Fig. 9a, b), indicating that these rocks were derived by partial melting of mélange rocks (Marschall and Schumacher, 2012; Nielsen and Marschall, 2017). Given the mélange contains both depleted (oceanic basalts and mantle wedge peridotites) and enriched (subducted sediments) components (Marschall and Schumacher, 2012), we thus suggest that the Jiaqiong andesites were produced by diapir partial melting of mélange rocks in a subduction zone.

#### 4.4. Deep geodynamic processes

As indicated above, the Jurassic magmatism along the BNSZ was caused by the northward subduction of the BNT oceanic lithosphere (Cao et al., 2019; Hu et al., 2020; Tang et al., 2019; Yang et al., 2021b; Zeng et al., 2016a; Zhang et al., 2017b). However, the detailed deep geodynamic processes responsible for the Middle Jurassic magmatism remain uncertain. The northward subduction of the BNT oceanic lithospheric slab beneath the southern Qiangtang subterrane at a normal or high dip angle and the subsequent arc magmatism during the Late Triassic have been revealed by the sedimentological and geochronological data from a north–south traverse across the BNSZ (Zeng et al., 2016b). However, the remnants of the Early Jurassic oceanic plateau have been identified within the BNTO (Zhang et al., 2014a, 2021), suggesting that oceanic slab probably dipped more shallowly or even subducted horizontally during this stage. This process is also supported by the contemporary arc magmatic gap in the southern Qiangtang subterrane (Li et al., 2016b; Yan et al., 2016a). During the Middle–Late Jurassic, renewed arc magmatism occurred widely along the northern of the BNSZ, probably triggered by the rollback of subducted oceanic slab, intra-oceanic subduction or oceanic ridge subduction (Li et al., 2020; Yan et al., 2016a; Yan and Zhang, 2020; Zhang et al., 2014a). Oceanic ridge subduction generally occurs in a relatively narrow range in a subduction zone and forms a typical rock suites, including adakite, high-Mg andesite, Nb-enriched basalt, oceanic island basalt (OIB) or mid-oceanic ridge basalt (MORB) (Tang et al., 2010; Wang et al., 2020). The absence of oceanic ridge subduction-related rock suites in the Jiaqiong–Amdo areas indicates that ridge subduction was unlikely to occur in the middle–eastern parts of the BNTO. However, the BNTO extends east–west for >2000 km, and the possibility of oceanic ridge subduction existed in other segments. Recently, Yan and Zhang (2020) proposed that arc magmatism was induced by intra-oceanic subduction in the BNTO during the Jurassic based on the Jurassic boninitic association and plateau lavas in the Zigaretangco–Namco areas. The magmatic rocks from the typical intra-oceanic arc, such as the Izu–Bonin–Mariana, the Aleutian, and the Lesser Antilles arc, generally have depleted isotopic compositions (Fig. 9a; Leat and Larer, 2003). However, the arc magmatic rocks show an enriched

Sr–Nd isotopic composition in study area (Fig. 9a, b; Tang et al., 2019; Zhang et al., 2021; Zeng et al., 2016a, 2016b), suggesting that these rocks were not generated by intra-oceanic subduction. In addition, boninite is generally regarded as the hallmark rock of forearc settings (e.g., Crawford et al., 1989; Li et al., 2013). Therefore, we suggest that the slab rollback model is more suitable for interpreting the deep geodynamic processes that led to the formation of the Jiaqiong andesites in this study, based on the following lines of evidence: (1) The Dong Co eclogites are the metamorphic product of the subducted BNT oceanic crust, suggesting a transition from flat to steep subduction during the Jurassic (Dong et al., 2016; Zhang et al., 2015, 2017b). During the process, upwelling asthenospheric mantle and hot corner flow caused by the slab rollback could have triggered the nearly simultaneous formation of the large volume of magmatic rocks, which is in agreement with the widespread occurrence of the Jurassic arc magmatic rocks along the BNSZ (Yan et al., 2016a; Zhu et al., 2016). (2) The ~177 Ma gabbros in the Amdo terrane were generated by the interaction between upwelling asthenospheric mantle and metasomatized lithospheric mantle, indicating the existence of a high-temperature magma source region during the Jurassic (Yan et al., 2016a). (3) Slab rollback would have induced vigorous mantle corner flow above the descending slab, leading to the retreat of the hinge and trenchward migration of the magmatic front (Gvirtzman and Nur, 1999; Schellart et al., 2006). Yan et al. (2016a) suggest that the gabbro–diorite–granodiorite associations from the Amdo terrane were generated by the asthenospheric upwelling caused by the rollback of the northward subducting BNTO during the Early–Middle Jurassic (177–174 Ma). In addition, the Middle–Late Jurassic andesitic rocks (165–158 Ma) were emplaced in the BNSZ to the south of the Amdo terrane, which were also formed in a subduction setting (Tang et al., 2019; Yang et al., 2021a). This southward migration of magmatism in a north–south section indicates the appearance of slab rollback during the Jurassic (Fig. 13). (4) Slab rollback can also lead to the extension and rifting within the overriding plate (e.g., Cassel et al., 2018). The Dongqiao ophiolite (188–181 Ma) is a typical SSZ-type ophiolite and was formed in an intra-oceanic arc–backarc basin, thus suggesting an extensional setting during the Early Jurassic (Liu et al., 2016; Wang et al., 2016). All the aforementioned evidence suggests that the Middle Jurassic Jiaqiong andesitic rocks were produced by partial melting of mélanges during slab rollback of the northward-subducting BNT oceanic lithospheric slab (Fig. 13). The asthenospheric upwelling and hot corner flow that were triggered by the slab rollback would have considerably heated and partially melted the physically mixed mélanges to produce the Jiaqiong andesites within the BNSZ (Hao et al., 2016, 2022; Marschall and Schumacher, 2012).

#### 4.5. Implications for the growth of the continental crust

It has been recognized that the continental crust is generated by magmatism in subduction zones (e.g., Cawood et al., 2009; Chen and Zhao, 2017; Hawkesworth et al., 2013; Kelemen and Behn, 2016). Phanerozoic continental crust grew mainly through both vertical addition by underplated magmas and lateral accretion of arc complexes and oceanic plateaus in subduction zones (e.g., Castro et al., 2013; Spencer et al., 2017; Wyman and Kerrich, 2009). Although the continental crust was consumed by the subduction erosion during subduction of the BNTO, the crustal vertical growth still had been identified (Hao et al., 2016; Yang et al., 2021b). Recent studies have shown that Jurassic mantle-derived andesitic magmas were emplaced in middle–upper crust, which is consistent with vertical crustal growth by magmatic underplating (Hu et al., 2020; Tang et al., 2019; Yan et al., 2016a; Yang et al., 2021a; Zeng et al., 2016a, 2016b). However, the origin of the

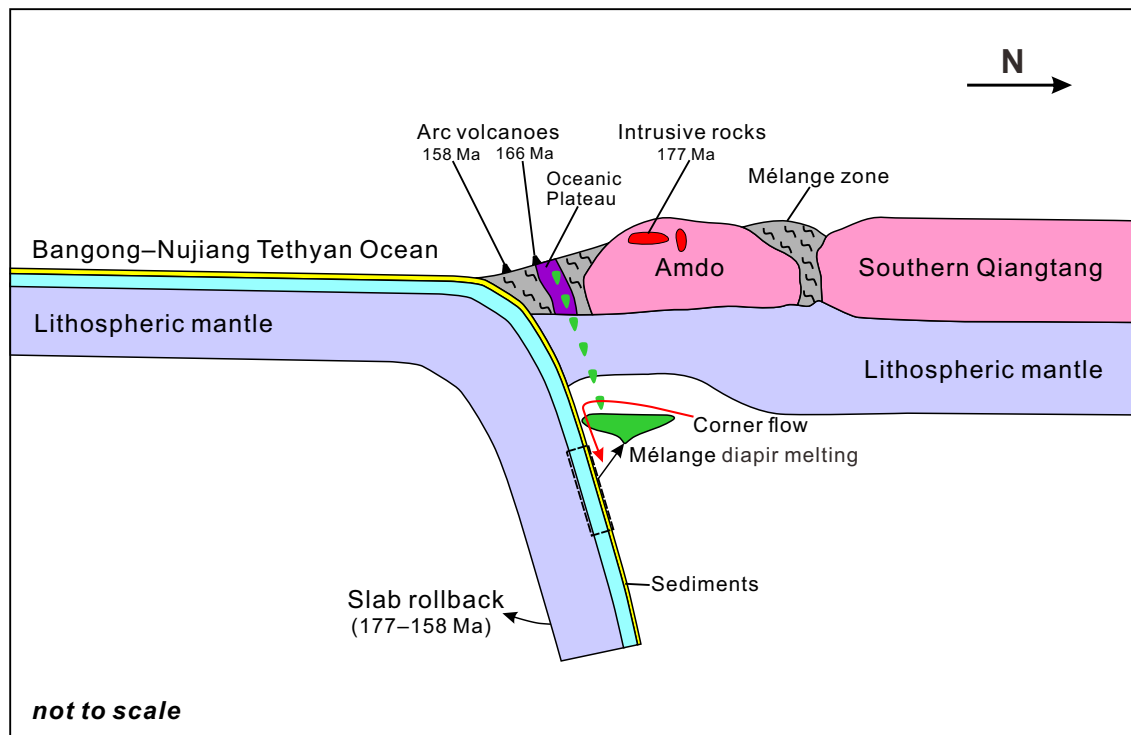


**Fig. 13.** Geodynamic model for the Jurassic arc magmatism along the southern Qiangtang subterrane. The model is based on concepts and data from Liu et al. (2016), Tang et al. (2019), Wang et al. (2016), Yan and Zhang (2020), Yang et al. (2021a), Zeng et al. (2016a), Zhang et al. (2012, 2014a, 2014b; 2021), and Zhong et al. (2017).

underplated magmas that drove this vertical growth is unknown. The Jiaqiong andesites in the middle–eastern parts of the BNSZ have variable  $\text{SiO}_2$  (52.0–65.9 wt%) and  $\text{MgO}$  (1.51–4.66 wt%) contents with moderate  $\text{Mg}^{\#}$  (35–63), similar to those of magmas in subduction-related magmatic arcs in middle–eastern parts of the southern Qiangtang margin (Fig. 8b; Hu et al., 2020; Tang et al., 2019; Zeng et al., 2016a, 2016b). Their REE and spider patterns are also similar to those of the average continental crust (Fig. 8a, b). The Jiaqiong andesites yield variable  $\text{MgO}$ , Cr, and Ni contents, initial  $^{87}\text{Sr}/^{86}\text{Sr}$  ratios, and  $\varepsilon_{\text{Nd}}(t)$  values, suggesting that these rocks were produced by partial melting of mélange rocks. Therefore, we suggest that the partial melting of mélange diapirs may contribute to the vertical growth of the continental crust in subduction zones.

## 5. Conclusions

(1) The Jiaqiong andesites were erupted at 169–164 Ma, and they are characterized by variable  $\text{MgO}$ , Cr, and Ni contents,  $(^{87}\text{Sr}/^{86}\text{Sr})_i$  ratios, and  $\varepsilon_{\text{Nd}}(t)$  values.

(2) The Jiaqiong andesites were most probably produced by partial melting of mélanges.

(3) The formation of the Jiaqiong andesites was triggered by asthenospheric upwelling and hot corner flow caused by the rollback of the northward subducting Bangong–Nujiang Tethyan oceanic lithospheric slab during the Middle Jurassic.

(4) Partial melting of mélanges provides an important support for the generation of andesitic magmas and vertical growth of the continental crust in subduction zones.

## CRediT authorship contribution statement

**Wan-Long Hu:** Conceptualization, Data curation, Investigation, Visualization, Writing – original draft. **Qiang Wang:** Conceptualization, Project administration, Data curation, Funding acquisition,

Investigation, Resources, Supervision, Writing – review & editing. **Jin-Hui Yang:** Conceptualization, Writing – review & editing. **Lu-Lu Hao:** Writing – review & editing. **Jun Wang:** Investigation, Writing – review & editing. **Yue Qi:** Investigation, Writing – review & editing. **Zong-Yong Yang:** Investigation. **Peng Sun:** Investigation.

## Declaration of Competing Interest

The authors declare that they have no known competing financial interests or personal relationships that could have appeared to influence the work reported in this paper.

## Acknowledgments

We thank Associate Editor Professor Zeming Zhang and two anonymous reviewers for their constructive and helpful comments on the manuscript. We also appreciate the assistance of Lin-Li Chen, Xin-Yu Wang, Sheng-Ling Sun, Xiang-Lin Tu, Wen Zeng, Yue-Heng Yang, and Le Zhang for the mineral composition, whole-rock element and Sr–Nd isotope, and zircon U–Pb dating and Lu–Hf isotope analyses. Financial support for this research was provided by the National Natural Science Foundation of China (42021002, 91855215 and 42102051), the Second Tibetan Plateau Scientific Expedition and Research (STEP) (2019QZKK0702) and the China Postdoctoral Science Foundation (2021M693189). This is contribution No. IS-3299 from GIGCAS.

## Appendix A. Supplementary data

Supplementary data to this article can be found online at <https://doi.org/10.1016/j.gr.2023.01.001>.

## References

- Barth, M.G., McDonough, W.F., Rudnick, R.L., 2000. Tracking the budget of Nb and Ta in the continental crust. *Chem. Geol.* 165, 197–213.
- Cai, Y.F., Wang, Y.J., Cawood, P.A., Zhang, Y.Z., Zhang, A.M., 2015. Neoproterozoic crustal growth of the Southern Yangtze Block: geochemical and zircon U-Pb geochronological and Lu-Hf isotopic evidence of Neoproterozoic diorite from the Ailaoshan zone. *Precambrian Res.* 266, 137–149.
- Cao, Y., Sun, Z., Li, H., Pei, J., Liu, D., Zhang, L., Ye, X., Zheng, Y., He, X., Ge, C., Jiang, W., 2019. New Paleomagnetic Results From Middle Jurassic Limestones of the Qiangtang terrane, Tibet: Constraints on the Evolution of the Bangong-Nujiang Ocean. *Tectonics* 38, 215–232.
- Cassel, E.J., Smith, M.E., Jicha, B.R., 2018. The impact of slab rollback on earth's surface: uplift and extension in the hinterland of the North American Cordillera. *Geophys. Res. Lett.* 45, 10996–11004.
- Castillo, P.R., Janney, P.E., Solidum, R.U., 1999. Petrology and geochemistry of Camiguin Island, southern Philippines: insights to the source of adakites and other lavas in a complex arc setting. *Contrib. Mineral. Petrol.* 134, 33–51.
- Castro, A., Vogt, K., Gerya, T., 2013. Generation of new continental crust by sublithospheric silicic-magma relamination in arcs: a test of Taylor's andesite model. *Gondwana Res.* 23 (4), 1554–1566.
- Cawood, P.A., Kröner, A., Collins, W.J., Kusky, T.M., Mooney, W.D., Windley, B.F., 2009. Accretionary orogens through Earth history. *Geol. Soc. Lond. Spec. Publ.* 318, 1–36.
- Chen, L., Zhao, Z.F., 2017. Origin of continental arc andesites: The composition of source rocks is the key. *J. Asian Earth Sci.* 145, 217–232.
- Class, C., Miller, D.M., Goldstein, S.L., Langmuir, C.H., 2000. Distinguishing melt and fluid subduction components in Umnak Volcanics, Aleutian Arc. *Geochim. Geophys. Geosyst.* 1 (6), 1004.
- Codillo, E.A., Le Roux, V., Marschall, H.R., 2018. Arc-like magmas generated by mélange-peridotite interaction in the mantle wedge. *Nat. commun.* 9 (1), 1–11.
- Crawford, A.J., Falloon, T.J., Green, D.H., 1989. Classification, petrogenesis and tectonic setting of boninites. In: Crawford, A.J. (Ed.), Boninites and Related Rocks. Unwin Hyman, London, pp. 1–49.
- Cruz-Uribe, A.M., Marschall, H.R., Gaetani, G.A., Le Roux, V., 2018. Generation of alkaline magmas in subduction zones by partial melting of mélange diapirs—An experimental study. *Geology* 46 (4), 343–346.
- DePaolo, D.J., 1981. Trace element and isotopic effects of combined wallrock assimilation and fractional crystallization. *Earth Planet. Sci. Lett.* 53, 189–202.
- Dong, Y.L., Wang, B.D., Zhao, W.X., Yang, T.N., Xu, J.F., 2016. Discovery of eclogite in the Bangong Co-Nujiang ophiolitic mélange, central Tibet, and tectonic implications. *Gondwana Res.* 35, 115–123.
- Fan, J.J., Li, C., Xie, C.M., Wang, M., Chen, J.W., 2015. Petrology and U-Pb zircon geochronology of bimodal volcanic rocks from the Maierze Group, northern Tibet: constraints on the timing of closure of the Bangong-Nujiang Ocean. *Lithos* 227, 148–160.
- Fan, J.J., Li, C., Xie, C.M., Liu, Y.M., Xu, J.X., Chen, J.W., 2017. Remnants of late Permian–Middle Triassic ocean islands in northern Tibet: implications for the late-stage evolution of the Paleo-Tethys Ocean. *Gondwana Res.* 44, 7–21.
- Fan, J.J., Li, C., Sun, Z.M., Xu, W., Wang, M., Xie, C.M., 2018. Early Cretaceous MORB-type basalt and A-type rhyolite in northern Tibet: Evidence for ridge subduction in the Bangong-Nujiang Tethyan Ocean. *J. Asian Earth Sci.* 154, 187–201.
- Fan, J.J., Niu, Y., Liu, Y.M., Hao, Y.J., 2021. Timing of closure of the Meso-Tethys Ocean: Constraints from remnants of a 141–135 Ma ocean island within the Bangong–Nujiang Suture Zone, Tibetan Plateau. *Geol. Soc. Am. Bull.* 133, 1875–1889.
- Farmer, M.J., Lee, C.T.A., Putirka, K.D., 2014. Mafic–felsic magma mixing limited by reactive processes: A case study of biotite-rich rinds on mafic enclaves. *Earth Planet. Sci. Lett.* 393, 49–59.
- Gibson, I.L., Kirkpatrick, R.J., Enneman, R., Schmincke, H.-U., Pritchard, G., Oakley, P.J., Thorpe, R.S., Marriner, G.F., 1982. The trace element composition of the lavas and dikes from a 3-km vertical section through the lava pile of Eastern Iceland. *J. Geophys. Res.* 87 (B8), 6532–6546.
- Grove, T., Parman, S., Bowring, S., Price, R., Baker, M., 2002. The role of an  $H_2O$ -rich fluid component in the generation of primitive basaltic andesites and andesites from the Mt. Shasta region, N California. *Contrib. Mineral. Petrol.* 142 (4), 375–396.
- Guo, Z., Wilson, M., Zhang, M., Cheng, Z., Zhang, L., 2013. Post-collisional, K-rich mafic magmatism in south Tibet: constraints on Indian slab-to-wedge transport processes and plateau uplift. *Contrib. Mineral. Petrol.* 165 (6), 1311–1340.
- Guynn, J.H., Kapp, P., Pullen, A., Heizler, M., Gehrels, G., Ding, L., 2006. Tibetan basement rocks near Armdo reveal “missing” Mesozoic tectonism along the Bangong suture, central Tibet. *Geology* 34, 505–508.
- Guynn, J., Kapp, P., Gehrels, G., Ding, L., 2012. U-Pb geochronology of basement rocks in central Tibet and paleogeographic implications. *J. Asian Earth Sci.* 43, 23–50.
- Gvirtzman, Z., Nur, A., 1999. The formation of Mount Etna as the consequence of slab rollback. *Nature* 401 (6755), 782–785.
- Gómez-Tuena, A., Straub, S.M., Zellmer, G.F., 2014. An introduction to orogenic andesites and crustal growth. *Geol. Soc. Lond. Spec. Publ.* 385, 1–13.
- Hao, L.L., Wang, Q., Wyman, D.A., Ou, Q., Dan, W., Jiang, Z.Q., Yang, J.H., Li, J., Long, X. P., 2016. Andesitic crustal growth via mélange partial melting: Evidence from Early Cretaceous arc dioritic/andesitic rocks in southern Qiangtang, central Tibet. *Geochem. Geophys. Geosyst.* 17 (5), 1641–1659.
- Hao, L.L., Wang, Q., Zhang, C., Ou, Q., Yang, J., Dan, W., Jiang, Z., 2019. Oceanic plateau subduction during closure of the Bangong-Nujiang Tethyan Ocean: Insights from central Tibetan volcanic rocks. *Geol. Soc. Am. Bull.* 131 (5–6), 864–880.
- Hao, L.L., Nan, X.Y., Kerr, A.C., Li, S.Q., Wu, Y.B., Wang, H., Huang, F., 2022. Mg-Ba-Sr-Nd isotopic evidence for a mélange origin of early Paleozoic arc magmatism. *Earth Planet. Sci. Lett.* 577, 117263.
- Harris, N.B.W., Xu, R.H., Lewis, C.L., Hawkesworth, C.J., Zhang, Y.Q., 1988. Isotope geochemistry of the 1985 Tibet Geotraverse, Lhasa to Golmud. *Phil. Trans. R. Soc. Lond. A Math. Phys. Sci.* 327 (1594), 263–285.
- Hastie, A.R., Kerr, A.C., Pearce, J.A., Mitchell, S.F., 2007. Classification of altered volcanic island arc rocks using immobile trace elements: development of the Th-Co discrimination diagram. *J. petrol.* 48 (12), 2341–2357.
- Hawkesworth, C.J., Kemp, A.I.S., 2006. Evolution of the continental crust. *Nature* 443 (7113), 811–817.
- Hawkesworth, C., Cawood, P., Dhuime, B., 2013. Continental growth and the crustal record. *Tectonophysics* 609, 651–660.
- Hoskin, P.W.O., Schaltegger, U., 2003. The Compositions of Zircon and Igneous and Metamorphic Petrogenesis. *Rev. Mineral. Geochem.* 53, 27–55.
- Hu, P.Y., Zhai, Q.G., Jahn, B.M., Wang, J., Li, C., Chung, S.L., Lee, H.Y., Tang, S., 2017. Late Early Cretaceous magmatic rocks (118–113Ma) in the middle segment of the Bangong–Nujiang suture zone, Tibetan Plateau: Evidence of lithospheric delamination. *Gondwana Res.* 44, 116–138.
- Hu, W.L., Wang, Q., Yang, J.H., Tang, G.J., Qi, Y., Ma, L., Yang, Z.Y., Sun, P., 2020. Amphibole and whole-rock geochemistry of early Late Jurassic diorites, Central Tibet: Implications for petrogenesis and geodynamic processes. *Lithos* 370–371, 105644.
- Hu, W.L., Wang, Q., Tang, G.J., Zhang, X.Z., Qi, Y., Wang, J., Ma, Y.M., Yang, Z.Y., Sun, P., Hao, L.L., 2022. Late Early Cretaceous magmatic constraints on the timing of closure of the Bangong–Nujiang Tethyan Ocean. *Central Tibet. Lithos* 416–417, 106648.
- Huang, Q.T., Li, J.F., Cai, Z.R., Xia, L.Z., Yuan, Y.J., Liu, H.C., Xia, B., 2015. Geochemistry, geochronology, Sr-Nd isotopic compositions of Jiang Tso ophiolite in the middle segment of the Bangong–Nujiang suture zone and their geological significance. *Acta Geol. Sin-Engl.* 89, 389–401.
- Jagoutz, O., Müntener, O., Schmidt, M.W., Burg, J.P., 2011. The roles of flux- and decompression melting and their respective fractionation lines for continental crust formation: evidence from the Kohistan arc. *Earth Planet. Sci. Lett.* 303, 25–36.
- Jones, R.E., Kirstein, L.A., Kasemann, S.A., Dhuime, B., Elliott, T., Litvak, V.D., Alonso, R., Hinton, R., Facility, E.I.M., 2015. Geodynamic controls on the contamination of Cenozoic arc magmas in the southern Central Andes: Insights from the O and Hf isotopic composition of zircon. *Geochim. Cosmochim. Acta* 164, 386–402.
- Jung, S., Hoernes, S., Mezger, K., 2002. Synorogenic melting of mafic lower crust: constraints from geochronology, petrology and Sr, Nd, Pb and O isotope geochemistry of quartz diorites (Damara orogen, Namibia). *Contrib. Mineral. Petro.* 143, 551–566.
- Kapp, P., DeCelles, P.G., 2019. Mesozoic-Cenozoic geological evolution of the Himalayan-Tibetan orogen and working tectonic hypotheses. *Am. J. Sci.* 319 (3), 159–254.
- Kelemen, P.B., Behn, M.D., 2016. Formation of lower continental crust by relamination of buoyant arc lavas and plutons. *Nat. Geosci.* 9 (3), 197–205.
- Lai, W., Hu, X., Garzanti, E., Xu, Y., Ma, A., Li, W., 2019. Early Cretaceous sedimentary evolution of the northern Lhasa terrane and the timing of initial Lhasa-Qiangtang collision. *Gondwana Res.* 73, 136–152.
- Leat, P.T., Larter, R.D., 2003. Intra-oceanic subduction systems: introduction. In: Larter, R.D., Leat, P.T. (Eds.), Intra-Oceanic Subduction Systems: Tectonic and Magmatic Processes, Vol. 219. Geol. Soc. London Spec. Publ., London, pp. 1–17.
- Lee, C.T.A., Bachmann, O., 2014. How important is the role of crystal fractionation in making intermediate magmas? Insights from Zr and P systematics. *Earth Planet. Sci. Lett.* 393, 266–274.
- Li, Y.B., Kimura, J., Machida, S., Ishii, T., Ishiwatari, A., Maruyama, S., Qiu, H.N., Ishikawa, T., Kato, Y., Haraguchi, S., Takahata, N., Hirahara, Y., Miyazaki, T., 2013. High-Mg Adakite and Low-Ca Boninite from a Bonin Forearc Seamount: Implications for the Reaction between Slab Melts and Depleted Mantle. *J. Petrol.* 54 (6), 1149–1175.
- Li, J.X., Qin, K.Z., Li, G.M., Richards, J.P., Zhao, J.X., Cao, M.J., 2014a. Geochronology, geochemistry, and zircon Hf isotopic compositions of Mesozoic intermediate-felsic intrusions in central Tibet: Petrogenetic and tectonic implications. *Lithos* 198–199, 77–91.
- Li, S.M., Zhu, D.C., Wang, Q., Zhao, Z.D., Sui, Q.L., Liu, S.A., Liu, D., Mo, X.X., 2014b. Northward subduction of Bangong–Nujiang Tethys: insight from Late Jurassic intrusive rocks from Bangong Tso in western Tibet. *Lithos* 205, 284–297.
- Li, S.M., Zhu, D.C., Wang, Q., Zhao, Z., Zhang, L.L., Liu, S.A., Chang, Q.S., Lu, Y.H., Dai, J. G., Zheng, Y.C., 2016a. Slab-derived adakites and subslab asthenosphere-derived OIB-type rocks at 156 ± 2 Ma from the north of Gerze, central Tibet: Records of the Bangong–Nujiang oceanic ridge subduction during the Late Jurassic. *Lithos* 262, 456–469.
- Li, Y., He, J., Han, Z., Wang, C., Ma, P., Zhou, A., Liu, S., Xu, M., 2016b. Late Jurassic sodium-rich adakitic intrusive rocks in the southern Qiangtang terrane, central Tibet, and their implications for the Bangong–Nujiang Ocean subduction. *Lithos* 245, 34–46.
- Li, S.M., Wang, Q., Zhu, D.C., Cawood, P.A., Stern, R.J., Weinberg, R., Zhao, Z.D., Mo, X. X., 2020. Reconciling orogenic drivers for the evolution of the Bangong–Nujiang Tethys during Middle-Late Jurassic. *Tectonics* 39 (2), e2019TC005951.

- Liu, D.L., Huang, Q.S., Fan, S.Q., Zhang, L.Y., Shi, R.D., Ding, L., 2014. Subduction of the Bangong-Nujiang Ocean: constraints from granites in the Bangong Co area. *Tibet. Geol. J.* 49, 188–206.
- Liu, T., Zhai, Q.G., Wang, J., Bao, P.S., Qiangba, Z., Tang, S.H., Tang, Y., 2016. Tectonic significance of the Dongqiao ophiolite in the north-central Tibetan plateau: Evidence from zircon dating, petrological, geochemical and Sr-Nd-Hf isotopic characterization. *J. Asian Earth Sci.* 116, 139–154.
- Liu, D.L., Shi, R.D., Ding, L., Huang, Q.S., Zhang, X.R., Yue, Y.H., Zhang, L.Y., 2017. Zircon U-Pb age and Hf isotopic compositions of Mesozoic granitoids in southern Qiangtang, Tibet: Implications for the subduction of the Bangong-Nujiang Tethyan Ocean. *Gondwana Res.* 41, 157–172.
- Marschall, H.R., Schumacher, J.C., 2012. Arc magmas sourced from mélange diapirs in subduction zones. *Nat. Geosci.* 5 (12), 862–867.
- Mitchell, A.L., Grove, T.L., 2015. Melting the hydrous, subarc mantle: the origin of primitive andesites. *Contrib. Mineral. Petrol.* 170 (2), 1–23.
- Morimoto, N., 1988. Nomenclature of pyroxenes. *Mineral. Petrol.* 39 (1), 55–76.
- Moyen, J.F., Laurent, O., Chelle-Michou, C., Couzinié, S., Vanderhaeghe, O., Zeh, A., Villars, A., Gardien, V., 2017. Collision vs. subduction-related magmatism: Two contrasting ways of granite formation and implications for crustal growth. *Lithos* 277, 154–177.
- Nielsen, S.G., Marschall, H.R., 2017. Geochemical evidence for mélange melting in global arcs. *Sci. adv.* 3 (4), e1602402.
- Pan, G.T., Wang, L.Q., Li, R.S., Yuan, S.H., Ji, W.H., Yin, F.G., Zhang, W.P., Wang, B.D., 2012. Tectonic evolution of the Qinghai-Tibet plateau. *J. Asian Earth Sci.* 53, 3–14.
- Petford, N., Atherton, M., 1996. Na-rich partial melts from newly underplated basaltic crust: the Cordillera Blanca Batholith. *Peru. J. Petrol.* 37, 1491–1521.
- Pichavant, M., Macdonald, R., 2007. Crystallization of primitive basaltic magmas at crustal pressures and genesis of the calc-alkaline igneous suite: experimental evidence from St Vincent, lesser Antilles arc. *Contrib. Mineral. Petrol.* 154, 535–558.
- Plank, T., Langmuir, C.H., 1993. Tracing trace elements from sediment input to volcanic output at subduction zones. *Nature* 362 (6422), 739–743.
- Plank, T., Langmuir, C.H., 1998. The chemical composition of subducting sediment and its consequences for the crust and mantle. *Chem. geol.* 145 (3–4), 325–394.
- Polat, A., Hofmann, A.W., 2003. Alteration and geochemical patterns in the 3.7–3.8 Ga Isua greenstone belt. West Greenland. *Precambrian Res.* 126, 197–218.
- Qu, X.M., Wang, R.J., Xin, H.B., Jiang, J.H., Chen, H., 2012. Age and petrogenesis of A-type granites in the middle segment of the Bangongnu-Nujiang suture, Tibetan plateau. *Lithos* 146, 264–275.
- Rapp, R.P., Watson, E.B., 1995. Dehydration melting of metabasalt at 8–32 kbar: Implications for continental growth and crust–mantle recycling. *J. Petrol.* 36, 891–931.
- Reubi, O., Blundy, J., 2009. A dearth of intermediate melts at subduction zone volcanoes and the petrogenesis of arc andesites. *Nature* 461, 1269–1274.
- Rocchi, S., Di Vincenzo, G., Dini, A., Petrelli, M., Vezzoni, S., 2015. Time-space focused intrusion of genetically unrelated arc magmas in the early paleozoic ross-delamerian orogen (morozumi range, antarctica). *Lithos* 232, 84–99.
- Rudnick, R.L., Gao, S., 2003. Composition of the continental crust. *Treatise on geochemistry* 3, 659.
- Rudnick, R.L., 1995. Making continental crust. *Nature* 378 (6557), 571–578.
- Schellart, W.P., Lister, G.S., Toy, V.G., 2006. A Late Cretaceous and Cenozoic reconstruction of the Southwest Pacific region: Tectonics controlled by subduction and slab rollback processes. *Earth Sci. Rev.* 76 (3–4), 191–233.
- Shimoda, G., Tatsumi, Y., Nohda, S., Ishizaka, K., Jahn, B.M., 1998. Setouchi high-Mg andesites revisited: geochemical evidence for melting of subducting sediments. *Earth Planet. Sci. Lett.* 160, 479–492.
- Spencer, C.J., Roberts, N.M.W., Santosh, M., 2017. Growth, destruction, and preservation of Earth's continental crust. *Earth Sci. Rev.* 172, 87–106.
- Stevenson, R., Henry, P., Gariépy, C., 1999. Assimilation-fractional crystallization origin of Archean Sanukitoid Suites: Western Superior Province. Canada. *Precambrian Res.* 96, 83–99.
- Straub, S.M., Gómez Gómez-Tuena, A., Stuart, F.M., Zellmer, G.F., Espinasa-Perena, R., Cai, Y., Iizuka, Y., 2011. Formation of hybrid arc andesites beneath thick continental crust. *Earth Planet. Sci. Lett.* 303, 337–347.
- Streck, M.J., Leeman, W.P., Chesley, J., 2007. High-magnesian andesite from Mount Shasta: A product of magma mixing and contamination, not a primitive mantle melt. *Geology* 35, 351–354.
- Sun, S.S., McDonough, W., 1989. Chemical and isotopic systematics of oceanic basalts: Implications for mantle composition and processes. *Geol. Soc. Lond. Spec. Publ.* 42, 313–345.
- Tang, G., Wang, Q., Wyman, D.A., Li, Z.X., Zhao, Z.H., Jia, X.H., Jiang, Z.Q., 2010. Ridge subduction and crustal growth in the Central Asian Orogenic Belt: Evidence from Late Carboniferous adakites and high-Mg diorites in the western Junggar region, northern Xinjiang (west China). *Chem. Geol.* 277 (3–4), 281–300.
- Tang, Y., Zhai, Q.G., Hu, P.Y., Xiao, X.C., Wang, H.T., Wang, W., Zhu, Z.C., Wu, H., 2019. Jurassic high-Mg andesitic rocks in the middle part of the Bangong-Nujiang suture zone, Tibet: New constraints for the tectonic evolution of the Meso-Tethys Ocean. *Acta Petrol. Sin.* 35, 3097–3114.
- Tatsumi, Y., Hanyu, T., 2003. Geochemical modeling of dehydration and partial melting of subducting lithosphere: Toward a comprehensive understanding of high-Mg andesite formation in the Setouchi volcanic belt, SW Japan. *Geochem. Geophys. Geosyst.* 4 (9), 1081.
- Tatsumi, Y., 2005. The subduction factory: How it operates in the evolving Earth. *GSA Today* 15 (7), 4–10.
- Taylor, S.R., McLennan, S.M., 1985. *The Continental Crust: Its Composition and Evolution*. Blackwell, Oxford.
- Wang, B.D., Wang, L.Q., Chung, S.L., Chen, J.L., Yin, F.G., Liu, H., Li, X.B., Chen, L.K., 2016. Evolution of the Bangong-Nujiang Tethyan ocean: insights from the geochronology and geochemistry of mafic rocks within ophiolites. *Lithos* 245, 18–33.
- Wang, Q., Tang, G.J., Hao, L.L., Wyman, D., Ma, L., Dan, W., Zhang, X.Z., Liu, J.H., Huang, T.Y., Xu, C.B., 2020. Ridge subduction, magmatism, and metallogenesis. *Sci. China Earth Sci.* 63 (10), 1499–1518.
- Wilson, B.M., 2007. *Igneous petrogenesis a global tectonic approach*. Springer Science & Business Media.
- Winchester, J.A., Floyd, P.A., 1977. Geochemical discrimination of different magma series and their differentiation products using immobile elements. *Chem. geol.* 20, 325–343.
- Wood, D.A., Joron, J.L., Treuil, M., 1979. A re-appraisal of the use of trace elements to classify and discriminate between magma series erupted in different tectonic settings. *Earth Planet. Sci. Lett.* 45 (2), 326–336.
- Wyman, D., Kerrich, R., 2009. Plume and arc magmatism in the Abitibi subprovince: implications for the origin of Archean continental lithospheric mantle. *Precambrian Res.* 168, 4–22.
- Yan, L.L., Zhang, K.J., 2020. Infant intra-oceanic arc magmatism due to initial subduction induced by oceanic plateau accretion: A case study of the Bangong Meso-Tethys, central Tibet, western China. *Gondwana Res.* 79, 110–124.
- Yan, H., Long, X., Wang, X.C., Li, J., Wang, Q., Yuan, C., Sun, M., 2016a. Middle Jurassic MORB-type gabbro, high-Mg diorite, calc-alkaline diorite and granodiorite in the Ando area, central Tibet: Evidence for a slab roll-back of the Bangong-Nujiang Ocean. *Lithos* 264, 315–328.
- Yan, M., Zhang, D., Fang, X., Ren, H., Zhang, W., Zan, J., Song, C., Zhang, T., 2016b. Paleomagnetic data bearing on the Mesozoic deformation of the Qiangtang Block: Implications for the evolution of the Paleo- and Meso-Tethys. *Gondwana Res.* 39, 292–316.
- Yang, P., Huang, Q., Zhou, R., Kapsiotis, A., Xia, B., Ren, Z., Cai, Z., Lu, X., Cheng, C., 2019. Geochemistry and geochronology of ophiolitic rocks from the Dongco and Lanong areas, Tibet: insights into the evolution history of the Bangong-Nujiang Tethys Ocean. *Minerals* 9 (8), 466.
- Yang, Z., Tang, J., Zhang, K., Zhao, X., Li, H., Wang, Y., Li, F., Ran, F., Huang, Y., 2021a. Southward subduction of the Bangong-Nujiang oceanic lithosphere triggered back-arc spreading: Evidence from the Late Jurassic Kongnongla magnesian andesites in central Tibet. *Lithos* 398–399, 106250.
- Yang, Z.Y., Wang, Q., Hao, L.L., Wyman, D.A., Ma, L., Wang, J., Yue, Q.I., Hu, W.L., 2021b. Subduction erosion and crustal material recycling indicated by adakites in central Tibet. *Geology* 49 (6), 708–712.
- Yin, A., Harrison, T.M., 2000. Geologic evolution of the Himalayan-Tibetan orogeny. *Annu. Rev. Earth Planet. Sci.* 28 (1), 211–280.
- Yogodzinski, G., Vervoort, J., Brown, S.T., Gerseny, M., 2010. Subduction Controls of Hf and Nd Isotopes in Lavas of the Aleutian Island Arc. *Earth Planet. Sci. Lett.* 300, 226–238.
- Zeng, Y.C., Chen, J.L., Xu, J.F., Wang, B.D., Huang, F., 2016a. Sediment melting during subduction initiation: Geochronological and geochemical evidence from the Darusto high-Mg andesites within ophiolite melange, central Tibet. *Geochim. Geophys. Geosyst.* 17, 4859–4877.
- Zeng, M., Zhang, X., Cao, H., Ettensohn, F.R., Cheng, W., Lang, X., 2016b. Late Triassic initial subduction of the Bangong-Nujiang Ocean beneath Qiangtang revealed: stratigraphic and geochronological evidence from Gaize. *Tibet. Basin Res.* 28, 147–157.
- Zhai, Q.G., Jahn, B.M., Wang, J., Hu, P.Y., Chung, S.L., Lee, H.Y., Tang, S.H., Tang, Y., 2016. Oldest Paleo-Tethyan ophiolitic mélange in the Tibetan Plateau. *Geol. Soc. Am. Bull.* 128 (3–4), 355–373.
- Zhang, K.J., Zhang, Y.X., Tang, X.C., Xia, B., 2012. Late Mesozoic tectonic evolution and growth of the Tibetan plateau prior to the Indo-Asian collision. *Earth Sci. Rev.* 114 (3–4), 236–249.
- Zhang, K.J., Xia, B., Zhang, Y.X., Liu, W.L., Zeng, L., Li, J.F., Xu, L.F., 2014a. Central Tibetan Meso-Tethyan oceanic plateau. *Lithos* 210–211, 278–288.
- Zhang, X., Shi, R., Huang, Q., Liu, D., Gong, X., Chen, S., Yi, G., Wu, K., Sun, Y., Ding, L., 2014b. Early Jurassic high-pressure metamorphism of the Amdo terrane, Tibet: Constraints from zircon U-Pb geochronology of mafic granulites. *Gondwana Res.* 26, 975–985.
- Zhang, Y.X., Li, Z.W., Zhu, L.D., Zhang, K.J., Yang, W.G., Jin, X., 2015. Newly discovered eclogites from the Bangong Meso-Tethyan suture zone (Gaize, central Tibet, western China): Mineralogy, geochemistry, geochronology, and tectonic implications. *Int. Geol. Rev.* 58 (5), 574–587.
- Zhang, K.J., Li, Q.H., Yan, L.L., Zeng, L., Lu, L., Zhang, Y.X., Hui, J., Jin, X., Tang, X.C., 2017a. Geochemistry of limestones deposited in various plate tectonic settings. *Earth Sci. Rev.* 167, 27–46.
- Zhang, X.Z., Wang, Q., Dong, Y.S., Zhang, C., Li, Q.Y., Xia, X.P., Xu, W., 2017b. High-pressure granulite facies overprinting during the exhumation of eclogites in the Bangong-Nujiang Suture Zone, central Tibet: Link to flat-slab subduction. *Tectonics* 36 (12), 2918–2935.
- Zhang, Y.X., Li, Z.W., Yang, W.G., Zhu, L.D., Jin, X., Zhou, X.Y., Tao, G., Zhang, K.J., 2017c. Late Jurassic-Early Cretaceous episodic development of the Bangong Meso-Tethyan subduction: Evidence from elemental and Sr-Nd isotopic geochemistry of arc magmatic rocks, Gaize region, central Tibet, China. *J. Asian Earth Sci.* 135, 212–242.
- Zhang, W.Q., Liu, C.Z., Liu, T., Zhang, C., Zhang, Z.Y., 2021. Subduction initiation triggered by accretion of a Jurassic oceanic plateau along the Bangong-Nujiang Suture in central Tibet. *Terra Nova* 33 (2), 150–158.

- Zheng, Y.F., Zhao, Z.F., 2017. Introduction to the structures and processes of subduction zones. *J. Asian Earth Sci.* 145, 1–15.
- Zheng, Y., Chen, Y., Dai, L., Zhao, Z., 2015. Developing plate tectonics theory from oceanic subduction zones to collisional orogens. *Sci. China. Ser. D.* 58 (7), 1045–1069.
- Zhong, Y., Liu, W.L., Xia, B., Liu, J.N., Guan, Y., Yin, Z.X., Huang, Q.T., 2017. Geochemistry and geochronology of the Mesozoic Lanong ophiolitic mélange, northern Tibet: Implications for petrogenesis and tectonic evolution. *Lithos* 292–293, 111–131.
- Zhu, D.C., Zhao, Z.D., Niu, Y., Mo, X.X., Chung, S.L., Hou, Z.Q., 2011. The Lhasa Terrane: record of a microcontinent and its histories of drift and growth. *Earth Planet. Sci. Lett.* 301, 241–255.
- Zhu, D.C., Zhao, Z.D., Niu, Y.L., Dilek, Y., Hou, Z.Q., Mo, X.X., 2013. The origin and pre-Cenozoic evolution of the Tibetan Plateau. *Gondwana Res.* 23, 1429–1454.
- Zhu, D.C., Li, S.M., Cawood, P.A., Wang, Q., Zhao, Z.D., Liu, S.A., Wang, L.Q., 2016. Assembly of the Lhasa and Qiangtang terranes in central Tibet by divergent double subduction. *Lithos* 245, 7–17.
- Zhu, Z., Zhai, Q., Hu, P., Chung, S., Tang, Y., Wang, H., Wu, H., Wang, W., Huang, Z., Lee, H., 2019. Closure of the Bangong-Nujiang Tethyan Ocean in the central Tibet: Results from the provenance of the Duoni Formation. *J. Sediment. Res.* 89 (10), 1039–1054.